Check for updates

Received: 5 January 2024 | Revised: 21 October 2024 | Accepted: 8 December 2024

DOI: 10.1111/bph.17449

RESEARCH ARTICLE

Silencing drug transporters in human primary muscle cells modulates atorvastatin pharmacokinetics: A pilot study

Emilia Hoste[1,2] | Louise Deldicque[3] | Giulio G. Muccioli[4] | Nadtha Panin[2] | Romano Terrasi[4] | Adrien Paquot[4] | Maxime Lingurski[1] | Sébastien Pyr dit Ruys[1] | Vincent Haufroid[2,5] | Laure Elens[1,2]

[1]Integrated PharmacoMetrics, PharmacoGenomics and PharmacoKinetics, Louvain Drug Research Institute (LDRI), Université catholique de Louvain (UCLouvain), Brussels, Belgium

[2]Louvain Centre for Toxicology and Applied Pharmacology, Institut de recherche expérimentale et clinique (IREC), Université catholique de Louvain (UCLouvain), Brussels, Belgium

[3]Institute of Neuroscience (IoNS), Université catholique de Louvain (UCLouvain), Louvain-la-Neuve, Belgium

[4]Bioanalysis and Pharmacology of Bioactive Lipids, Louvain Drug Research Institute (LDRI), Université catholique de Louvain (UCLouvain), Brussels, Belgium

[5]Department of Clinical Chemistry, Cliniques universitaires Saint-Luc, Brussels, Belgium

Correspondence
Laure Elens, Integrated PharmacoMetrics, PharmacoGenomics and PharmacoKinetics, Louvain Drug Research Institute (LDRI), Université catholique de Louvain (UCLouvain), Avenue Emmanuel Mounier 72, B1.72.02 1200 Brussels, Belgium.
Email: laure.elens@uclouvain.be

Funding information
This work was supported by Fonds pour la Formation à la Recherche dans l''Industrie et dans l''Agriculture (FRIA) under the Grant Number FC33437 and by the Bourse du Patrimoine (01150164) to Emilia Hoste E., and by grants from the Fonds national de la Recherche scientifique ([FRS-FNRS)] (Grants J018317 and J006920).

Background and Purpose: Non-adherence to atorvastatin treatment is relatively common and partly due to statin-related myotoxicities (SRMs). The risk of developing SRM is dose- and concentration-dependent, highlighting the importance of atorvastatin pharmacokinetics. This study explored the inter-individual variabilities in expression of the atorvastatin transporter gene contributing to modulation of atorvastatin within the muscle cell.

Experimental Approach: mRNA levels of efflux and influx transporters were measured and modulated with siRNAs to evaluate effects on intracellular accumulation of atorvastatin in primary cultures of differentiated myotubes from 12 human volunteers.

Key Results: All genes assessed were expressed with a high inter-individual variability. In differentiated myotubes, efflux transporters were expressed at higher levels than the influx carriers. When considering efflux and influx transporters separately, *ABCC1* and *SLCO2B1* are the most highly expressed efflux and influx transporters. Suppression of *ABCC1*, *ABCC4* and/or *ABCG2* mRNA levels with siRNA significantly increased intracellular accumulation of atorvastatin in differentiated myotubes. Interestingly, the siRNA targeting *ABCG2* had a moderate effect on intracellular accumulation of atorvastatin in a volunteer expressing the *ABCG2* variant rs2231142 (c.421C>A, p.Gln141Lys). This hypothesis was further validated in a HEK recombinant model overexpressing ABCG2 either wild-type (421C) or variant (421A). Reduction of *SLCO1B1* and *SLCO2B1* mRNA levels significantly modified intracellular accumulation of atorvastatin in only some volunteers, depending on the expression levels of transporters.

Conclusion and Implications: Silencing *ABCC1*, *ABCC4* or *ABCG2* expression alters accumulation of atorvastatin in myotubes, whereas the effect of silencing influx transporters depends on the expression of these transporters.

KEYWORDS
efflux transporter, influx transporter, inhibitors, inter-individual variability, primary human skeletal muscle cell cultures

Abbreviations: AA, antibiotic–antimycotic; CFDA, 5[6]-carboxyfluorescein diacetate succinimidyl ester; CV, coefficient of variation; DM, differentiation medium; PK, pharmacokinetics; PM, proliferation medium; SRMs, statin-related myotoxicities.

Vincent Haufroid and Laure Elens contributed equally to this work.

 © 2025 British Pharmacological Society.

1 | INTRODUCTION

Atorvastatin has shown high efficacy to lower the risk of cardiovascular disease development via the reduction of high cholesterol blood levels (European Society of Cardiology [ESC], 2022). However, the number of non-compliant patients can vary from 24% in secondary prevention to 43% in primary prevention within 24 months of treatment and even increase up to 56% within a 12-year time window (Turner et al., 2020; Voora et al., 2022). The main cause of discontinuation is the occurrence of muscle side effects (Stroes et al., 2015). Diverse mechanisms of atorvastatin-related muscle toxicity have been highlighted but remain incompletely clarified. As an **HMG-CoA reductase** inhibitor, atorvastatin competitively inhibits the **mevalonate** pathway involved in **cholesterol** synthesis (Baker, 2005). Along with its therapeutic activity, this inhibition of HMG-CoA reductase mediated by atorvastatin also accounts for its adverse effects, including the muscular complaints. Indeed, the atorvastatin-mediated inhibition of the mevalonate pathway and the consequent downstream depletion of metabolites lead to a joint reduction of their respective physiological activity that might constitute one of the possible explanations for atorvastatin-related muscular side effects (Sakamoto et al., 2007). Atorvastatin-mediated HMG-CoA reductase inhibition and the resulting metabolite depletion are known to be dose- and plasma concentration-dependent (Adams et al., 2012). This suggests that understanding the intracellular pharmacokinetics (PK) of atorvastatin is essential in order to identify the reasons for the variabilities in treatment response and in the susceptibility to muscle side effects. In particular, the fact that statin-related myotoxicity (SRM) is specific to skeletal muscle tissue and is dependent on dose and drug potency (Morikawa et al., 2005; Norata et al., 2014; Ownby & Hohl, 2002) provides a rationale to explore the importance of factors affecting the intra-myocyte concentrations of statins.

To date, most of the available studies on the PK of atorvastatin have investigated the systemic effect of specific natural genetic variations on its PK profiles and/or singular susceptibility for the development of muscle side effects. Clinical studies have consistently demonstrated that the rs4149056 single nucleotide polymorphism in *SLCO1B1* (c.521T>C, p.Val174Ala) decreases atorvastatin hepatic uptake, associates with high systemic exposure to atorvastatin and increases the risk of muscular side effects (Birmingham et al., 2015; Stillemans et al., 2022; Turner et al., 2020; Turongkaravee et al., 2021). Interestingly, studies using recombinant cell models have also demonstrated that ***ABCC1*** and *SLCO2B1* might play important roles in explaining the modulation of atorvastatin accumulation at the cellular level (Hoste et al., 2023; Knauer et al., 2010), while a case–control pharmacogenetic study highlighted a potential role of the ***ABCG2*** variant rs2231142 (c.421C>A, p.Gln141Lys) in explaining a part of the susceptibility to develop muscle discomfort in patients (Mirošević Skvrce et al., 2015). Investigating how influx and efflux transporters modulate the intracellular accumulation of atorvastatin in primary cultures of skeletal muscle tissue, based on the differential expression levels of the transporters, might provide new insights into understanding this issue. This is particularly relevant because it has been demonstrated that the ratio of **atorvastatin lactone**-to-atorvastatin acid in muscle tissue is correlated with the risk of developing statin-induced muscle side-effects (Lauritzen et al., 2023; Skottheim et al., 2011). As atorvastatin lactone is more lipophilic compared to the acid form, it easily crosses biological membranes by passive diffusion, whereas the distribution of the acid form is thought to be modulated by active influx and efflux transporters (Preta, 2022). Hence, understanding the mechanisms of the accumulation of atorvastatin acid within the muscle cell appears to be one of the key components.

Altogether, the published data provide evidence of the involvement of influx and efflux transporters in the systemic PK of atorvastatin. However, few data are available with regard to their expression in the muscle tissue and their specific contribution to local accumulation of atorvastatin within the muscle cells. Our study thus explored the relative expression of influx (*SLCO1B1*, *SLCO1B3* and *SLCO2B1*) and efflux (*ABCC1*, ***ABCC2***, ***ABCC4*** and *ABCG2*) transporters of atorvastatin in primary cultures of differentiated human myotubes and the consequences of transporter-specific expression modulations, taking into consideration selected genetic variations, on the intracellular

What is already known

- High atorvastatin-lactone-to- atorvastatin-acid ratio in muscle correlates with increased risk of statin-induced muscle side effects.
- Intracellular accumulation of ATV and its systemic pharmacokinetics are modulated by influx and efflux transporters.

What does this study add

- Drug transporter expression in myotubes varies among individuals, with higher efflux than influx transporters expression.
- Silencing *ABCC1*, *ABCC4* and/or *ABCG2* altered atorvastatin myotube accumulation, while silencing influx transporters had moderate effects.

What is the clinical significance

- Using ABCC1-, ABCC4- or ABCG2-inhibitors with atorvastatin may increase atorvastatin-induced side-effects by modulating muscle accumulation.
- Pharmacogenetics and/or cooperation between influx and efflux transporters might modulate the effect of transporter inhibition.

14765381, 0, Downloaded from https://bpspubs.onlinelibrary.wiley.com/doi/10.1111/bph.17449 by Bibliothecaire En Chef Uni Catholique De Louvain (Ucl), Wiley Online Library on [25/02/2025]. See the Terms and Conditions (https://onlinelibrary.wiley.com/terms-and-conditions) on Wiley Online Library for rules of use; OA articles are governed by the applicable Creative Commons License

accumulation of atorvastatin. Knowing the individual factors explaining the singular susceptibility for developing muscle discomfort could assist the clinician in anticipating potential compliance problems with atorvastatin therapy, with dosing adaptation or alternative therapeutic strategies.

2 | METHODS

2.1 | Human skeletal muscle cell primary cultures

The Hospitalo-Facultaire Saint-Luc—UCLouvain Ethical Committee approved the protocols for the collection and use of human tissue (reference 2020/06OCT/488) which were conducted in accordance with the Declaration of Helsinki. All subjects gave fully informed and written consent. The human primary differentiated myotube cultures used in the present study were derived from vastus lateralis muscle biopsies from 12 male volunteers (mean age: 29 ± 9 years, body mass index [BMI]: 27.2 ± 4.1 $kg{\cdot}m^{-2}$) and collected as described previously (De Groote et al., 2021).

The biopsies were cryopreserved at −80°C in a fetal bovine serum (FBS):dimethyl sulfoxide (DMSO) mix (90:10, v/v). For the isolation of satellite cells, a part of the muscle biopsy (15–20 mg) was thawed on ice in a 35-mm Petri dish (Corning, NY) in sterile conditions. The biopsy was then cut into small pieces, then transferred in a new 35-mm Petri dish and gently covered with a drop of Matrigel® (Corning) before incubation for 30 min at 37°C with 5% CO_2. Two millilitres of complete media (Dulbecco's modified Eagle's medium [DMEM] with high glucose, no pyruvate supplemented with 20% FBS, 0.5% Ultroser G [Sartorius, Göttingen, Germany] and 4 mM of HEPES [Sigma-Aldrich]) were subsequently added to the Petri dish. Once long filaments were observed at the periphery of the explants, the medium was discarded and the explants were detached using 2.5 ml of dispase (0.8 $U{\cdot}ml^{-1}$)/collagenase (0.1 $U{\cdot}ml^{-1}$) (Sigma-Aldrich) for 2 h at 37°C. The cell pellet was then washed twice in medium (DMEM with high glucose, no pyruvate supplemented with 20% FBS and 1% antibiotic–antimycotic [AA] [Thermo Fisher Scientific]) before being resuspended in 10 ml of proliferation medium (PM) (DMEM with high glucose, no pyruvate supplemented with 20% FBS, 1% AA and 0.5% Ultroser G) and seeded in a 100-mm Petri dish (Corning).

After proliferation, the myoblasts were sorted using magnetic-activated cell sorting (MACS; Miltenyi Biotec, Bergisch Gladbach, Germany, Cat# 130-042-501) with magnetic microbeads directly linked to CD56. For this purification step, the cells were incubated for 30 min at 37°C in 4 ml of medium (DMEM with high glucose and no pyruvate supplemented with 0.5% bovine serum albumin [BSA] [0.22 µm filtered]) containing the antibody anti-CD56 diluted 1/1000 (BD Biosciences, Franklin Lakes, NJ, Cat# 559043, RRID:AB_397180). The cells were then detached with cell dissociation buffer (Thermo Fisher Scientific), and after centrifugation at 200 x *g* for 5 min at room temperature, the pellet was washed with 8 ml of phosphate-buffered saline (PBS) supplemented with 0.5% BSA and 2-mM EDTA. After centrifugation at 200 x *g* for 5 min at room temperature, the supernatant was discarded and the pellet was resuspended in 80 µl of PBS–BSA–EDTA to which 20 µl of the secondary antibody anti-mouse IgG microbeads was added to be diluted 1/5 (Miltenyi Biotec, Cat# 130-048-402, RRID:AB_244361) and incubated at 4°C for 15 min. The cells were then washed with 8 ml of medium and resuspended in 500 µl of PBS–BSA–EDTA. For the purification, the labelled cells were added to the sterile LS columns (Miltenyi Biotec, Cat# 130-042-401) of the MACS magnetic support. After three steps of washing, satellite cells retained in the column were mechanically detached using the adapted syringe. The purified myoblasts were eventually seeded in 8 ml of PM into a new 100-mm Petri dish.

When needed, cells were regularly split or frozen before reaching full confluency using cell dissociation buffer. Briefly, after 13 min of incubation at 37°C with cell dissociation buffer, 3 ml of PBS containing 2-mM EDTA was added to dissociate the cells, along with 3 ml of PM for cell dissociation buffer neutralization. The entire content was then transferred to a 15-ml tube and centrifuged at 200 x *g* for 5 min at room temperature. After discarding the supernatant, the cell pellet was resuspended in 10 ml of PM and seeded in new 100-mm Petri dishes to allow proliferation. Cells were then frozen in 1-ml cryotubes composed of FBS and DMSO (90:10, v/v) at −80°C.

Once thawed prior to the experiments, cells were seeded in a 100-mm Petri dish for proliferation and then seeded in 35-mm Petri dishes. At full confluency, the PM was replaced by a differentiation medium (DM) (DMEM with high glucose, no pyruvate supplemented with 1% AA and 2% FBS). This medium, low in serum, is known to promote the fusion of myoblasts into a network of myotubes. The experiments were performed on fully differentiated myotubes, 7 days after the start of the differentiation.

2.2 | HEK293 recombinant cell culture

The cell lines were developed according to the method described in the supporting information. Transfected human embryonic kidney cells (HEK293; ATCC, Cat# CRL-1573, RRID:CVCL_0045) were grown in DMEM with high glucose, L-glutamine and sodium pyruvate (Gibco, BRL) supplemented with 10% (v/v) FBS and 1% (v/v) penicillin–streptomycin (Thermo Fisher Scientific, Waltham, MA) in the presence of the selection antibiotic hygromycin (0.5 $mg{\cdot}L^{-1}$). The cells were cultured at 37°C and 5% CO_2. For reculturing, the cells were detached with enzyme-free cell dissociation buffer (Thermo Fisher Scientific).

2.3 | Quantitative polymerase chain reaction (qPCR) analysis

The total RNA was extracted in 1 ml of TRIzol (TriPure®, Sigma-Aldrich) according to the manufacturer's protocol. The purified RNA was quantified using the EzDrop100 from Blue-Ray Biotech (New Taipei City, Taiwan). The reverse transcription was performed using 1 µg of RNA per condition with the kit GoScript Reverse Transcriptase (Promega, Madison, WI) on a Bio-Rad iCycler Thermal Cycler iQ5

14765381, 0, Downloaded from https://bpspubs.onlinelibrary.wiley.com/doi/10.1111/bph.17449 by Bibliothecaire En Chef Uni Catholique De Louvain (Ucl), Wiley Online Library on [25/02/2025]. See the Terms and Conditions (https://onlinelibrary.wiley.com/terms-and-conditions) on Wiley Online Library for rules of use; OA articles are governed by the applicable Creative Commons License

Multicolor Real-Time PCR (Hercules, CA) according to the manufacturer's instructions. Real-time qPCR analysis was performed in 96-well plates using SsoAdvanced Universal SYBR Green Supermix on the CFX96 Touch™ device and software from Bio-Rad. Accurate quantification of gene copies per sample was achieved by simultaneously running calibration curves and the samples in triplicate, enabling the precise determination of gene copy numbers. Normalization was carried out using the reference gene beta-2-microglobulin (B2M). The purity of the PCR product was confirmed by analysing the melt curve conducted at the end of the analysis. The detailed sequences of the forward and reverse primers targeting the human genes of interest can be found in Table 1 (Eurofins Scientific SE, Ebersberg, Germany).

2.4 | Proteomic profiling

On the last day of the myotubes' differentiation, the medium was removed. After centrifugation at 200 x *g* for 5 min at room temperature, the washed pellet was resuspended in 25 µl of lysis buffer. The lysis buffer was composed of sodium deoxycholate (0.5%), triethylammonium bicarbonate (50 mM), NaCl (150 mM), IGEPAL (CA-630) (1%), SDS (0.1%) and dodecyl maltoside (0.2%) adjusted to a pH between 7.2 and 7.5 and containing the cOmplete™ Protease Inhibitor Cocktail purchased from Roche (Basel, Switzerland). Before digestion, quantification of the total protein content was performed with the use of a Bradford assay purchased from Thermo Fisher Scientific, according to the supplier's protocol. The samples were treated according to the protocol defined in the HYGIEIA project (Ward et al., 2022).

2.5 | Western blot

The Immuno-related procedures used comply with the recommendations made by the *British Journal of Pharmacology* (Alexander et al., 2018). The medium was discarded from the culture dish, and cells were detached with cell dissociation buffer and washed using ice-cold PBS. Lysis was performed by adding 50 µl of lysis buffer containing protease inhibitors (see Section 2.4) to the cell pellet. Samples were then centrifuged at 10,000 *g* for 20 min, and the supernatant was collected in a fresh tube and placed on ice. A small volume of the lysate was used to perform the total protein quantification assay. In a total volume of 30 µl, total protein content was normalized to 10 µg per sample with 3 µl of reducing agent and 7.5 µl of NuPAGE LDS Sample Buffer 4× (Thermo Fisher Scientific). The samples were heated for 10 min at 70°C on a thermoblock. For electrophoresis, samples were loaded on a NuPAGE 4%–12% Bis–Tris 1.5-mm Mini Protein Gel (Invitrogen) in a MOPS running buffer using an XCell SureLock chamber for 1 h at 175 V. The membranes were then soaked subsequently in methanol and then transferred to a buffer containing 20% methanol. Transfer was performed using a polyvinylidene fluoride (PVDF) transfer membrane (Cat# 88518, Thermo Fisher Scientific) by assembling the transfer sandwich. The cassette was placed in the transfer XCell SureLock tank according to the manufacturer's instructions. The transfer was performed during 1 h10 at 30 V. After transfer, the membranes were rinsed three times in 10 ml of Tris-buffered saline (TBS) 0.05% Tween 20 with agitation and then immersed in 10 ml of EveryBlot Blocking Buffer (Bio-Rad) and placed on a rocker for 5 min at room temperature. The antibodies, monoclonal anti-ABCG2 clone EPR20080 (IgG, Abcam, Cat# ab207732, RRID:AB_3674120) or monoclonal anti-MRP4 clone EPR20403 (IgG, Abcam, Cat# ab233382, RRID:AB_36674121), both produced in rabbits, were freshly diluted in 10 ml of EveryBlot Blocking Buffer, both at a dilution ratio of 1/2500. As indicated in the datasheet of these antibodies, the exact immunogen sequence used to generate this antibody is proprietary information of Abcam. Membranes were placed on a rocker and incubated with the primary antibody solution overnight at 4°C. Membranes were then washed three times with 10 ml of TBS 0.05% Tween 20 for 5 min on an agitator. The secondary antibody (goat anti-rabbit IgG-HRP (Abcam, Cat# ab205718, RRID:AB_2819160) was freshly diluted in 10 ml of EveryBlot Blocking Buffer (Bio-Rad) at a dilution ratio of 1/2500, and membranes were placed in the secondary antibody solution on a rocker for 1 h at room temperature and then rinsed three times in 10 ml of TBS 0.05% Tween 20 with agitation. The revelation was performed with Immobilon Classico Western HRP Substrate (Merck), and membranes were visualized on an Amersham Imager.

TABLE 1 Forward and reverse primers targeting the human genes of interest.

Genes	Forward primers	Reverse primers
ABCC1	ACTGAATGGCATCACCTTCTC	ACTGAATGGCATCACCTTCTC
ABCC2	CCTCATTCAGACGACCATCC	ATTCTCAATGCCAGCTTCCT
ABCC4	AAAATGTACGCCTGGGAAAAG	GGTGAAGGTCACAAACACGA
ABCG2	CAGGACTCAATGCAACAGGA	TTCAGGTAGGCAATTGTGAGG
Beta-2-microglobulin (*B2M*)	ATGAGTATGCCTGCCGTGTGA	GGCATCTTCAAACCTCCATG
Myogenin (*MyoG*)	ATAACGCGGCCTCTAATTCC	ATCGGGAAGAGACCAGAACA
Myosin (*MYH2*)	GTGCTGTACAACCTCAAAGAAC	CTCGGGCTTATACACAGGCA
SLCO1B1	ACTGATTCTCGATGGGTTGG	TTCCAGCACATGCAAAGAC
SLCO1B3	AATTTGGACATGCAAGACAATG	AGTGAAAGACCAGGAACACCTC
SLCO2B1	GCTGCCATCCCCTACTTCTT	CTAGGCCATCCTGCTTCTTC

14765381, 0, Downloaded from https://bpspubs.onlinelibrary.wiley.com/doi/10.1111/bph.17449 by Bibliothecaire En Chef Uni Catholique De Louvain (Ucl), Wiley Online Library on [25/02/2025]. See the Terms and Conditions (https://onlinelibrary.wiley.com/terms-and-conditions) on Wiley Online Library for rules of use; OA articles are governed by the applicable Creative Commons License

2.6 | Immunofluorescence

A total of 50,000 cells (differentiated myotubes or HEK293 cells) were seeded in an ibidi eight-well µSilde precoated with poly-L-lysine (Cat# 80806, Proxylab). After seeding, cells were incubated at 37°C with 5% CO_2. After 2 days, the medium was removed, and cells were washed with 150 µl of PBS for 10 min and then fixed with 4% paraformaldehyde during 20 min. Next, cells were washed three times with 150 µl of PBS for 10 min and permeabilized with 0.25% saponin for 5 min. Blocking was then performed during 30 min with 200 µl of PBS containing 1% BSA and 0.25% saponin. The supernatant was discarded, and cells were incubated for 1 h with the PerCP-y™ 5.5 Mouse Anti-Human CD388 Antibody (BD Biosciences, Cat# 561460, RRID:AB_10714098) at a final dilution of 1/100 in PBS 0.1% BSA containing 1/1000 Phalloidin-iFluor 488 Reagent (Abcam) to stain the cytoskeleton (for myotubes). Cells were then washed twice for 10 min with PBS 0.1% BSA. Mounting was performed using four drops of the ibidi mounting medium with 4′,6-diamidino-2-phenylindole (DAPI) (Cat# 50011, Proxylab). Cells were finally visualized using an ECHO Revolve R4 microscope with appropriate filters (i.e., DAPI—excitation [EX]: 380/30 and emission [EM]: 450/50, FITC—EX: 470/40 and EM: 525/50, and CY5—EX: 630/40 and EM: 700/75 for blue, green and red fluorescence, respectively). Of note, the contribution from autofluorescence was eliminated by reducing the exposure time and fluorescence gain with unstained cells.

2.7 | Control of the differentiation

The appearance and morphology of the myoblasts and the myotubes were observed and controlled through the bright-field microscope Leitz Labovert (Leica Microsystems, Wetzlar, Germany). The pictures were taken with Zeiss AxiomCam MRc (Zeiss, Oberkochen, Germany) at the end of the proliferation and at different stages of the differentiation. In parallel, RNA extraction of the samples was performed as described above, at both the end of the proliferation and differentiation. *MyoG* and *MYH2* (see primers in Table 1) mRNA levels at the two stages were quantified. The calibration curves for each gene transcript enabled the precise quantification of gene copies in each sample that were further normalized on the B2M expression levels.

2.8 | Gene silencing

Silencer™ Pre-Designed siRNAs targeting *ABCC1* (Cat# 4390824), ABCC4 (Cat# AM16708), *ABCG2* (Cat# 4392420), *SLCO1B1* (Cat# 4392420) and *SLCO2B1* (Cat# AM16708), as well as the negative control (siRNA scramble, Cat# 4390843), were purchased from Thermo Fisher Scientific. siRNAs were resuspended in nuclease-free water at a concentration of 10 µM. The protocol of siRNA transfection has been optimized by testing different timings (and combination of timings) of transfection. As shown in Figure S1, the best gene silencing results were obtained with double siRNA transfection performed at Days 2 and 4 after myoblast differentiation initiation. siRNA transfection was performed with 5 µl of Lipofectamine™ RNAiMAX (Thermo Fisher Scientific) in 35-mm Petri dishes, following the manufacturer's instructions. The siRNAs were diluted 400-fold to achieve a recommended final concentration of 25 nM in the wells.

2.9 | Atorvastatin accumulation experiments

2.9.1 | Myotubes

On the last day of the differentiation, the media were removed and replaced with 1350 µl of fresh DM to which 150 µl of atorvastatin was added for a final concentration of 5, 7.5 or 15 nM in the Petri dish. Of note, these concentrations were selected based on a clinical study conducted in a cohort of ambulatory patients treated with atorvastatin, where plasma concentrations ranged from approximately 0.15 to 30 nM, depending on the dose and the time after drug intake (Stillemans et al., 2022). In the conditions with the inhibitors, the myotubes were incubated for 15 min prior to the addition of atorvastatin with **MK-571**, CFDA or **erlotinib** at final concentrations of 25, 20 and 25 µM, respectively (Tivnan et al., 2015). The cells were incubated for 2 h at 37°C with 5% CO_2. At the end of the incubation, the Petri dishes were placed on ice, the media were removed, and the cells were washed twice with 1 ml of ice-cold PBS. Atorvastatin was then extracted according to the protocol described in the following section.

2.9.2 | HEK293 cells

One day before the accumulation experiment, 500,000 cells were seeded in poly-L-lysine-precoated 12-well plates in DMEM containing 10% FBS. On the day of the experiment, the media were removed and replaced with a fresh medium containing atorvastatin at a final concentration of 50 nM. For inhibition with Ko-**143**, cells were preincubated for 15 min with Ko-143 at a concentration of 1 µM prior to the addition of atorvastatin. The cells were incubated for 2 h at 37°C with 5% CO_2. At the end of the incubation, the plates were placed on ice, the media were removed, and the cells were washed twice with 1 ml of ice-cold PBS. Atorvastatin was then extracted according to the protocol described in the following section.

2.10 | Extraction and quantification of atorvastatin

Extraction of atorvastatin contained in the myotubes was directly performed in the 35-mm Petri dishes using 350 µl of MeOH:H_2O (60:40, v/v) containing d5-atorvastatin (used as an internal standard) at a final concentration of 5 nM. The extracted cells were then transferred to an Eppendorf tube and subsequently sonicated for 5 s (Vibra-Cell™, Sonics, CT) before being centrifuged at 10,500 *g* for 7 min at 4°C; 300 µl of the supernatant was ultimately collected into a new 1.5 mL Eppendorf tube for the dosage. For protein normalization, 10 µl of the

14765381, 0, Downloaded from https://bpspubs.onlinelibrary.wiley.com/doi/10.1111/bph.17449 by Bibliothecaire En Chef Uni Catholique De Louvain (Ucl), Wiley Online Library on [25/02/2025]. See the Terms and Conditions (https://onlinelibrary.wiley.com/terms-and-conditions) on Wiley Online Library for rules of use; OA articles are governed by the applicable Creative Commons License

supernatant was used to perform Pierce™ BCA protein quantification according to the manufacturer's instructions. Atorvastatin was quantified by cation high-performance liquid chromatography–tandem mass spectrometry (HPLC-MS/MS), performed on an Acquity UPLC class H coupled to Xevo TQ-S (Waters, Milford, MA), as previously described (Hoste et al., 2023).

2.11 | Genotyping

Genetic testing on differentiated myotubes was performed using the SOPHiA GENETICS® Community Panel for Pharmacogenomics, which is a targeted, capture-based next-generation sequencing (NGS) panel, including 41 pharmacogenes, developed and tested in collaboration with the RNPGx (French-speaking network of pharmacogenetics) according to the instructions of the manufacturer on a MiSeq platform (Illumina®). The laboratory has also an ISO15189 certification for the clinical use of this panel.

In addition, the variants rs45511401 (c.2012G>T, p.Gly671Val) in *ABCC1* (Cat# C__25614373_30) and rs12422149 (c.935G>A, p.Arg312Gln) in *SLCO2B1* (Cat# C___3101331_10) were identified in the volunteers using TaqMan assays (Thermo Fisher Scientific). The experiment was performed in 96-well plates, according to the manufacturer's protocol.

2.12 | Data and statistical analysis

The data and statistical analysis comply with the recommendations of the *British Journal of Pharmacology* on experimental design and analysis in pharmacology (Curtis et al., 2022). Declared group sizes reflected the number of values used for statistical analysis (one data point per experiment), and all statistical analyses were conducted on these independent values only (technical replicates were excluded from consideration as independent values). Where applicable, experiments were designed to generate equal group sizes using blinded analysis. However, for secondary endpoint analyses involving chemical inhibition, group sizes were unequal due to the nature of the control setup across multiple independent experiments. For accumulation experiments, we normalized the responses of individual wells to the corresponding controls to reduce the unwanted sources of variation, and data were expressed as '% accumulation relative to controls'. Graphs and statistical analysis were performed on GraphPad Prism Version 9 (La Jolla, CA). For assays to determine the intracellular accumulation of atorvastatin, statistical significance was assessed using one- or two-way ANOVA; a post hoc Tukey's comparison was performed only if F in ANOVA achieved a P value less than 0.05 and there was no significant variance inhomogeneity. A paired t test was used for the comparison of expression levels before and after siRNA treatment, and correlations were performed with non-parametric Spearman correlation analysis. In any case, the threshold for statistical significance was set at $P < 0.05$. All experiments were performed at least three times in three replicates ($n = 9$), with the exception of the measurement of atorvastatin variability in the 12 volunteers that was performed only once ($n = 3$) due to a lack of biological material and logistical constraints. Accordingly, no statistical test was performed to assess the inter-volunteer differences in atorvastatin accumulation. As the silencing of *SLCO1B1* mRNA expression failed in one experiment (i.e., from S5), we excluded accumulation data derived from this experiment. Therefore, for the *SLCO1B1* silencing experiment, the number of independent values was $n = 6$. Additionally, for the correlation analysis, data from one of the 12 volunteers were excluded due to being identified as an extreme value and given only one replicate was available for this particular volunteer. Power analysis was performed using G*Power software (Version 3.1, Universität Kiel, Kiel, Germany) (Faul et al., 2007). For the correlation analysis between intracellular atorvastatin concentrations and transporter expression levels, with a total sample size of 12 volunteers, a typical two-sided type I error of 0.05 (α) and a power of 0.80 ($\pi = 1 - \beta$), our design theoretically allowed us to reject the null hypothesis of rho = 0 if the actual correlation was characterized by a rho value greater than |0.6|. For the ANOVA analysis considering gene silencing experiments, our design included three selected volunteers in three experimental replicates with nine independent values and between three (chemical inhibition) and five (gene silencing) experimental conditions. With a typical two-sided type I error of 0.05 (α) and a power of 0.80 ($\pi = 1 - \beta$), our design theoretically allowed us to detect an effect size (∂) ranging from 0.81 to 1.13. Data are reported as means ± SD, unless otherwise specified. Proteomic analysis was performed on DIA-NN software (Demichev et al., 2020).

2.13 | Materials

Atorvastatin calcium salt and d5-atorvastatin calcium salt were both purchased from Alsachim (Illkirch-Graffenstaden, France). **MK-571** sodium salt hydrate, 5[6]-carboxyfluorescein diacetate succinimidyl ester (CFDA), **erlotinib** and **Ko-143** were all purchased from Sigma-Aldrich (St. Louis, MO).

2.14 | Nomenclature of targets and ligands

Key protein targets and ligands in this article are hyperlinked to corresponding entries in http://www.guidetopharmacology.org and are permanently archived in the Concise Guide to PHARMACOLOGY 2021/22 (Alexander et al., 2021).

3 | RESULTS

3.1 | Myoblast differentiation

3.1.1 | Microscopy

Bright-field microscopy images showed the evolution from myoblast proliferation (Figure 1a, Panel A) to differentiation into myotubes

14765381, 0, Downloaded from https://bpspubs.onlinelibrary.wiley.com/doi/10.1111/bph.17449 by Bibliothecaire En Chef Uni Catholique De Louvain (Ucl), Wiley Online Library on [25/02/2025]. See the Terms and Conditions (https://onlinelibrary.wiley.com/terms-and-conditions) on Wiley Online Library for rules of use; OA articles are governed by the applicable Creative Commons License

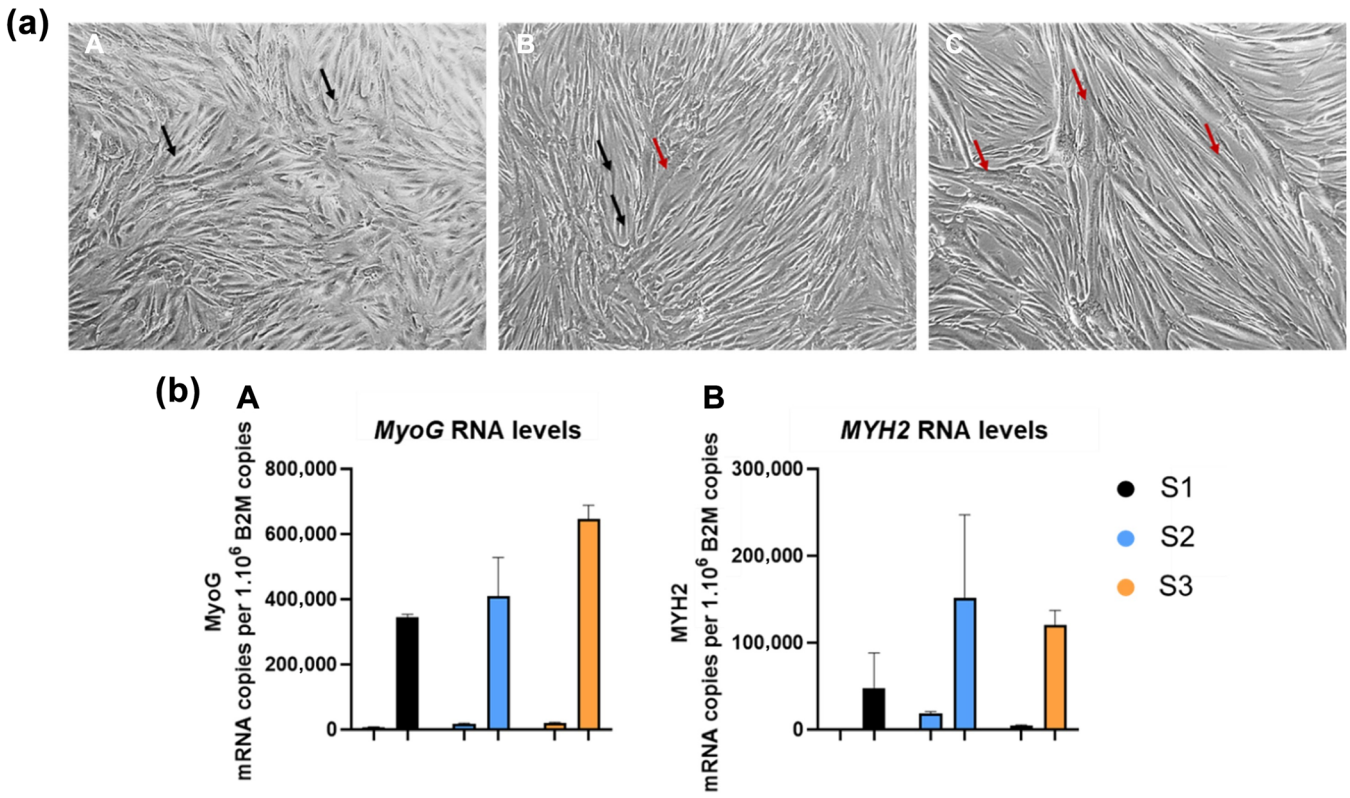


FIGURE 1 Control of the differentiation by (a) bright-field microscopy (A) during the proliferation stage, (B) during the differentiation process (Days 3 and 4) and (C) differentiated myotubes on the last day of the differentiation (Day 7). Black arrows indicate mononucleated myoblasts, while red arrows show multinucleated myotubes. Control of the differentiation by (b) RT-qPCR representing the mRNA levels of (A) *MyoG* and of (B) *MYH2* of three volunteers (S1–S3) at the stage of proliferation and differentiation. The mRNA expression levels are expressed in copies of the gene per 1.10^6 B2M copies (n = 9).

(Figure 1a, Panels B and C). At the proliferation stage (Figure 1a, Panel A), the myoblasts (black arrows) were mononucleated. On the third to fourth day of the differentiation (Figure 1a, Panel B), while single myoblasts were still visible (black arrows), the process of fusion into myotubes had started (red arrow). On the last day of the differentiation (Figure 1a, Panel C), all myoblasts had fused to form a network of myotubes (red arrows). Visual inspection was conducted before initiating any experiment to ensure proper myoblast differentiation.

3.1.2 | Expression of the differentiation genes

To further confirm the differentiation of myoblast into myotubes, mRNA expression of *MyoG* and of *MYH2* were quantified by RT-qPCR (Figure 1b). Whereas *MyoG* is a transcriptional factor promoting genes that are specific to the skeletal muscle, *MYH2* is involved in the development of functional skeletal muscle fibres (UniProt Consortium, 2023). Monitoring their expression at the end of the differentiation of the myotubes is thus complementary and ensures that differentiation had occurred. The mRNA expression levels of both *MyoG* and *MYH2* were increased at the end of the process of differentiation when compared to their mRNA expression levels during proliferation (Figure 1b). The transcript was quantified in each experiment to confirm myotube differentiation.

3.2 | Expression of efflux and influx transporters in the skeletal muscle tissue

3.2.1 | Transporter expression in differentiated myotubes

Screening of the mRNA expression levels for the major described efflux (*ABCC1*, *ABCC2*, *ABCC4* and *ABCG2*) and influx (*SLCO2B1*, *SLCO1B1* and *SLCO1B3*) transporters for atorvastatin was performed in the 12 volunteers after myotube differentiation (Figure 2). Among efflux transporters (Figure 2a), the mRNA expression levels of *ABCC1* were the highest, followed by *ABCG2* and by *ABCC4*, whereas *ABCC2* was characterized by the lowest relative mRNA levels. ABC transporter mRNA levels were also assessed in the original quadriceps biopsy of 7 out of the 12 volunteers (Figure S2). While *ABCC1* remains the most expressed efflux transporter, there are differences in the mRNA expression patterns of *ABCC4* and *ABCG2* between uncultured muscle biopsies and cultured differentiated myotubes because in the

14765381, 0, Downloaded from https://bpspubs.onlinelibrary.wiley.com/doi/10.1111/bph.17449 by Bibliothecaire En Chef Uni Catholique De Louvain (Ucl), Wiley Online Library on [25/02/2025]. See the Terms and Conditions (https://onlinelibrary.wiley.com/terms-and-conditions) on Wiley Online Library for rules of use; OA articles are governed by the applicable Creative Commons License

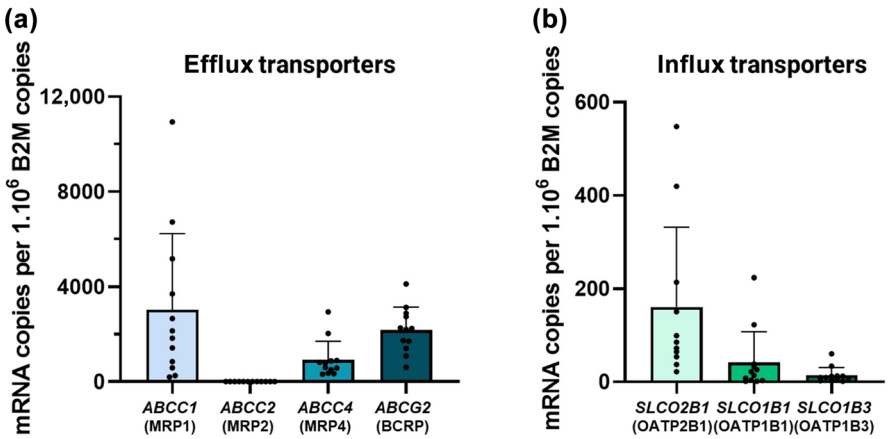


FIGURE 2 mRNA expression levels for (a) efflux transporters (*ABCC1*, *ABCC2*, *ABCC4* and *ABCG2*) and (b) influx transporters (*SLCO2B1*, *SLCO1B1* and *SLCO1B3*). Each point represents the mRNA value quantified in total RNA extracts obtained from differentiated myotubes generated from a biopsy of a given volunteer (n = 12). Data are reported as mRNA copies of the gene per 1.10^6 B2M copies.

uncultured material, *ABCC4* seems to be relatively more expressed than *ABCG2*, whereas in the cultured myotubes, the opposite was observed.

Among influx transporters in cultured myotubes (Figure 2b), *SLCO2B1* showed the highest relative mRNA levels followed by *SLCO1B1*. The mean mRNA levels of *SLCO1B3* were the lowest among the influx transporters assessed. We were unable to assess the mRNA levels of influx transporters in the original biopsies due to a lack of material.

For all transporters assessed, a high inter-individual variability in the mRNA expression levels in the cultured myotubes was observed with a coefficient of variation (CV) ranging from 44.2% for *ABCG2* to 160.9% for *SLCO1B1*, with the CV for *ABCC1* and *SLCO2B1* CV being 86% and 106.4%, respectively. The variability in efflux transporter mRNA expression appeared to be similar in the original biopsy.

In parallel, we also assessed the protein expression level by DIA shotgun proteomics in cultured myotubes. Only ABCC1 and ABCC4 proteins were detected in differentiated myotube extracts, probably because the presence of the proteins in the samples is below the detection limit of our system. Nevertheless, our results indicate a significant correlation between mRNA and protein levels for both transporters (Spearman $r = 0.7010$ and 0.6891, $P = 0.011$ and 0.013 for ABCC1 and ABCC4, respectively; see Figure S3), suggesting that mRNA expression levels provided a good reflection of the protein pool of the transporters, at least for ABCC1 and ABCC4, that were among the most highly expressed.

3.2.2 | Levels of the intracellular accumulation of atorvastatin and correlation with transporter expression

A preliminary screening of the accumulation of atorvastatin in differentiated myotubes was performed by incubating the cells with 15 nM of atorvastatin. A relatively large variability in intracellular atorvastatin levels was observed among the volunteers (CV = 22.2%) (Figure 3). We next evaluated the correlations between the intracellular levels of atorvastatin and the expression levels of the different transporters. A significant correlation was observed between the intracellular levels of atorvastatin and the mRNA expression levels of *ABCC1* (Figure 3b). However, the correlation between intracellular atorvastatin and ABCC1 protein levels showed only a non-significant trend (Figure 3c). No significant correlation was found with any other single efflux or influx transporters (Spearman *r* ranging from −0.356 to −0.08515 and $P > 0.05$ for *ABCC4* and *SLCO2B1*, respectively).

3.3 | Effects of transporter activity on atorvastatin accumulation

Inhibition of the efflux proteins was assessed using a general MRP inhibitor, namely, MK-571. MK-571 co-incubation significantly increased the intracellular accumulation of atorvastatin, in comparison to the control condition (Figure 4). The effects of chemical inhibition of influx transport was also assessed through different inhibitors. OATP1B1/1B3 inhibition was investigated with CFDA and showed no significant effects on atorvastatin intracellular accumulation in cultured myotubes (Figure 4). OATP2B1 inhibition in cultured myotubes was assessed with erlotinib (25 μM) and was associated with a decrease in accumulation (Figure 4).

3.4 | Effects of transporter expression modulation on intracellular accumulation of atorvastatin

3.4.1 | Efflux transporters

Volunteer selection and modulation of ABCC1, ABCG2 and ABCC4 expression

Three volunteers (hereafter called S1–S3) showing high, intermediate or low basal ABC transporter mRNA expression levels covering the entire range were selected from the 12 volunteers in order to carry out gene silencing on *ABCC1*, *ABCC4* or *ABCG2* or dual *ABCC1*–*ABCG2* and subsequent experiments to assess atorvastatin accumulation. Data related to basal expression of mRNA for all investigated transporters, in those three volunteers are shown in Figure 5. Cultured primary myotubes from S2 showed the highest mRNA and

14765381, 0, Downloaded from https://bpspubs.onlinelibrary.wiley.com/doi/10.1111/bph.17449 by Bibliothecaire En Chef Uni Catholique De Louvain (Ucl), Wiley Online Library on [25/02/2025]. See the Terms and Conditions (https://onlinelibrary.wiley.com/terms-and-conditions) on Wiley Online Library for rules of use; OA articles are governed by the applicable Creative Commons License

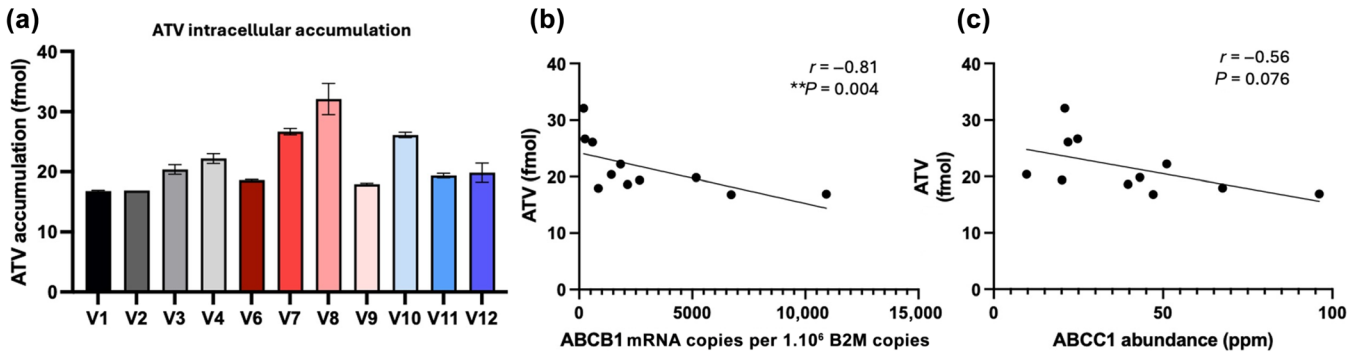


FIGURE 3 (a) Intracellular accumulation of atorvastatin (ATV) in 11 out of the 12 volunteers (n = 3 except for V2 where n = 1 due to a lack of material); V5 was removed from the analysis as the value obtained was considered as an outlier (Figure S4). Correlation between intracellular accumulation of atorvastatin and *ABCC1* (b) mRNA and (c) protein expression levels.

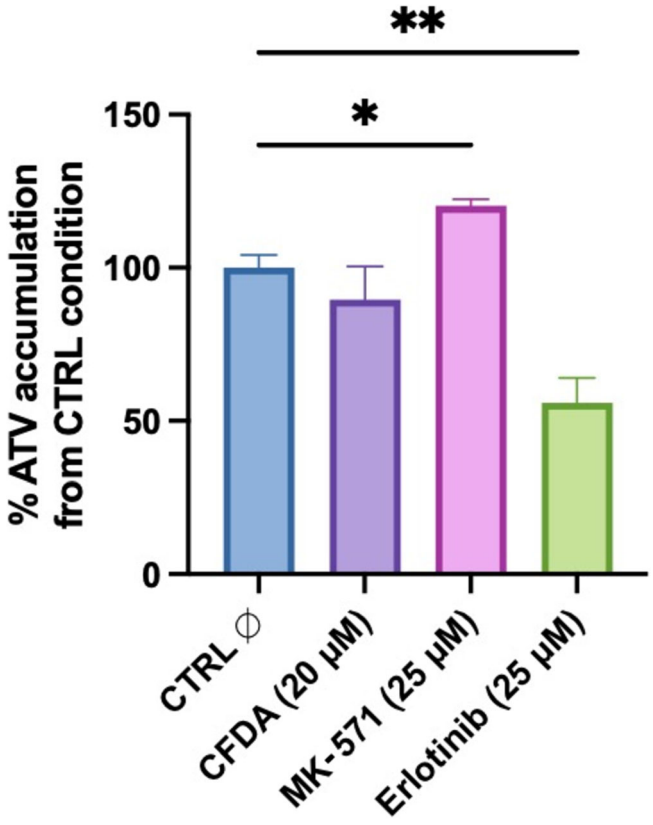


FIGURE 4 Effect of chemical inhibition of transporters on intracellular accumulation of atorvastatin. Intracellular levels of atorvastatin (ATV) relative to control (CTRL). CFDA, treatment with 5 [6]-carboxyfluorescein diacetate succinimidyl ester at 20 µM; CTRL Ø, no treatment; Erlotinib, treatment with erlotinib at 25 µM; MK-571, treatment with MK-571 at 25 µM. n = 21 for CFDA, n = 9 for MK-571 and n = 3 for erlotinib inhibition experiments. *P<0.05, **P<0.01, significantly different as indicated. No statistical analysis was performed on conditions where n < 5 (erlotinib).

protein levels of ABCC1, followed by cells from S1 and S3 (Figures 5a and S5a), while *ABCG2* mRNA was higher in cells from S1, followed by S3 and S2 whose mRNA levels were the lowest among the three selected volunteers (Figure 5a). As explained above, ABCG2 protein levels could not be quantified as they were below the limit of detection of our proteomic method, but ABCG2 protein could be detected by immunofluorescence (Figure 5c) and Western blot (Figure S5c). Despite immunofluorescence providing non-quantitative expression data, the images confirm a higher expression of ABCG2 for volunteers S1 and S3 compared to S2, as the red signal appears slightly stronger for these volunteers, which aligns with our mRNA quantification (Figure 5a) results. For all three genes, siRNA strongly reduced the mRNA levels when compared to the basal expression (Figure 5a). This drop in mRNA levels was also observed at the protein level after treatment of the cells with siRNA for ABCC1, ABCC4 and ABCG2 (Figure S5).

Effects of ABCC1 and/or ABCG2 gene silencing on intracellular accumulation of atorvastatin

Treatment with either *ABCC1* or *ABCG2* siRNA significantly increased the intracellular accumulation of atorvastatin in differentiated myotubes cultured from the three volunteers' biopsies, when compared to the control condition (Figure 6b, Panels A–C, and Figure S6a). Interestingly, the increase observed in the intracellular accumulation of atorvastatin after *ABCC1* siRNA treatment was more pronounced in cells from S2, who were characterized by the highest level of *ABCC1* expression, compared to S1 or S3 (Figure 6b). Also, the increase in atorvastatin intracellular levels was significantly higher after *ABCC1* siRNA treatment when compared to treatment with siRNA *ABCG2*, especially in S3, where ABCG2 siRNA treatment had only a minor effect on the intracellular levels of atorvastatin. Interestingly, S3 was a heterozygous carrier of the reduced-of-function *ABCG2* variant rs2231142 (c.421C>A, p.Gln141Lys). However, S2 did also carry the *ABCG2* variant allele, and the increase in intracellular atorvastatin after *ABCG2* treatment was even more important when compared to S1 who was homozygous wild-type (WT) for this variant.

We further investigated the effect of ABCC1 and ABCG2 dual silencing (Figure 6b, Panels A–C) and observed that the increase in atorvastatin accumulation was greater than the effect of *ABCC1* or *ABCG2* silencing alone, except in myotubes cultured from S2, which is

14765381, 0, Downloaded from https://bpspubs.onlinelibrary.wiley.com/doi/10.1111/bph.17449 by Bibliothecaire En Chef Uni Catholique De Louvain (Ucl), Wiley Online Library on [25/02/2025]. See the Terms and Conditions (https://onlinelibrary.wiley.com/terms-and-conditions) on Wiley Online Library for rules of use; OA articles are governed by the applicable Creative Commons License

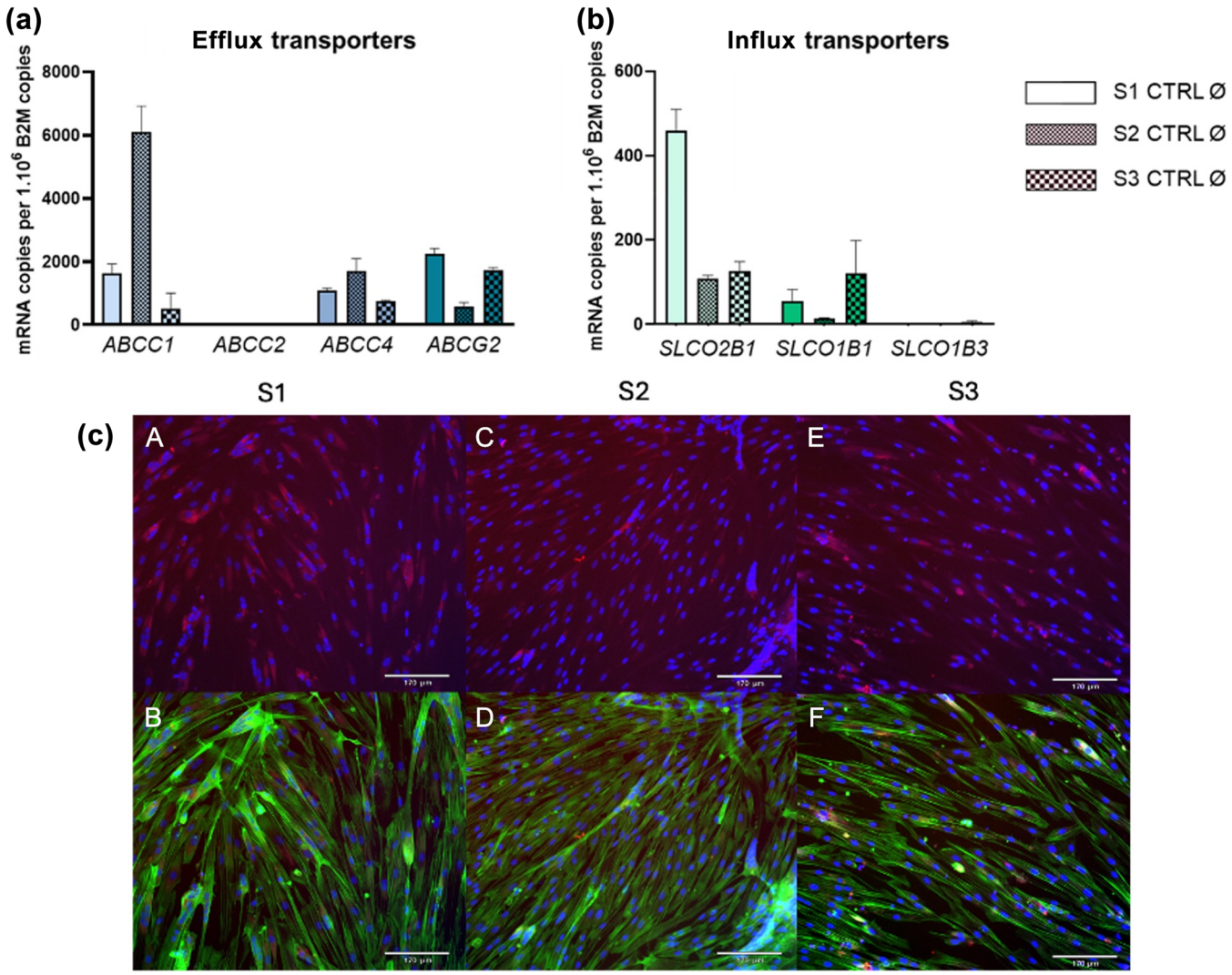


FIGURE 5 Basal mRNA expression of the transporters in control conditions in the volunteers S1–S3 for (a) the efflux transporters and (b) influx transporters. (c) Immunofluorescence images (20×) of cultured myotubes for (A, B) S1, (C, D) S2 and (E, F) S3. (A, C, E) overlay of DAPI nucleus (blue) with PecP ABCG2 (red) staining. (B, D and F) overlay of DAPI nucleus (blue), PerCP-y™ 5.5-ABCG2 (red) and Phalloidin 488 cytoskeleton (green) staining.

characterized by the highest expression levels of ABCC1 and also ABCC4 and carries the *ABCG2* variant allele.

Finally, we assessed the effects of silencing ABCC4 and showed that suppression of ABCC4 was associated with a substantial increase in atorvastatin accumulation in all three selected volunteers (Figures 6c and S6b).

Treatment of the myotubes with Lipofectamine or siRNA scramble significantly reduced efflux transporter mRNA levels without affecting the mRNA levels of influx transporters (Figure S7). The reduced expression observed on efflux transporters was however less important than the effect induced by the specific siRNAs. Furthermore, treatment of the cells with Lipofectamine alone or transfection with the scrambled siRNA had no effects on either ABCC1 and ABCC4 peptide levels or atorvastatin intracellular accumulation (Figures S8 and S9). These results confirm that the reduced efflux transporter expression induced by siRNA scramble transfection or Lipofectamine was not sufficient to affect the intracellular accumulation of atorvastatin and that the effect of *ABCC1* or *ABCG2* siRNA treatment on atorvastatin intracellular levels is specific.

Effects of ABCG2 overexpression and genetic variant on intracellular accumulation of atorvastatin in a recombinant HEK model

A HEK293 recombinant model overexpressing ABCG2 stably transfected with a plasmid containing either the WT (HEK ABCG2 WT) or the variant (HEK ABCG2 variant) *ABCG2* allele was developed. HEK293 control cells consisted of cells transfected with the empty vector (HEK pCMV). ABCG2 expression was assessed by immunofluorescence (Figure 7a–c) and Western blot (Figure S10). Results confirmed a high ABCG2 expression in both HEK ABCG2 WT and variant and no or weak basal protein expression in HEK pCMV. When the cells were incubated with 50-nM atorvastatin, intracellular accumulation was significantly decreased in HEK293 cells overexpressing

14765381, 0, Downloaded from https://bpspubs.onlinelibrary.wiley.com/doi/10.1111/bph.17449 by Bibliothecaire En Chef Uni Catholique De Louvain (Ucl), Wiley Online Library on [25/02/2025]. See the Terms and Conditions (https://onlinelibrary.wiley.com/terms-and-conditions) on Wiley Online Library for rules of use; OA articles are governed by the applicable Creative Commons License

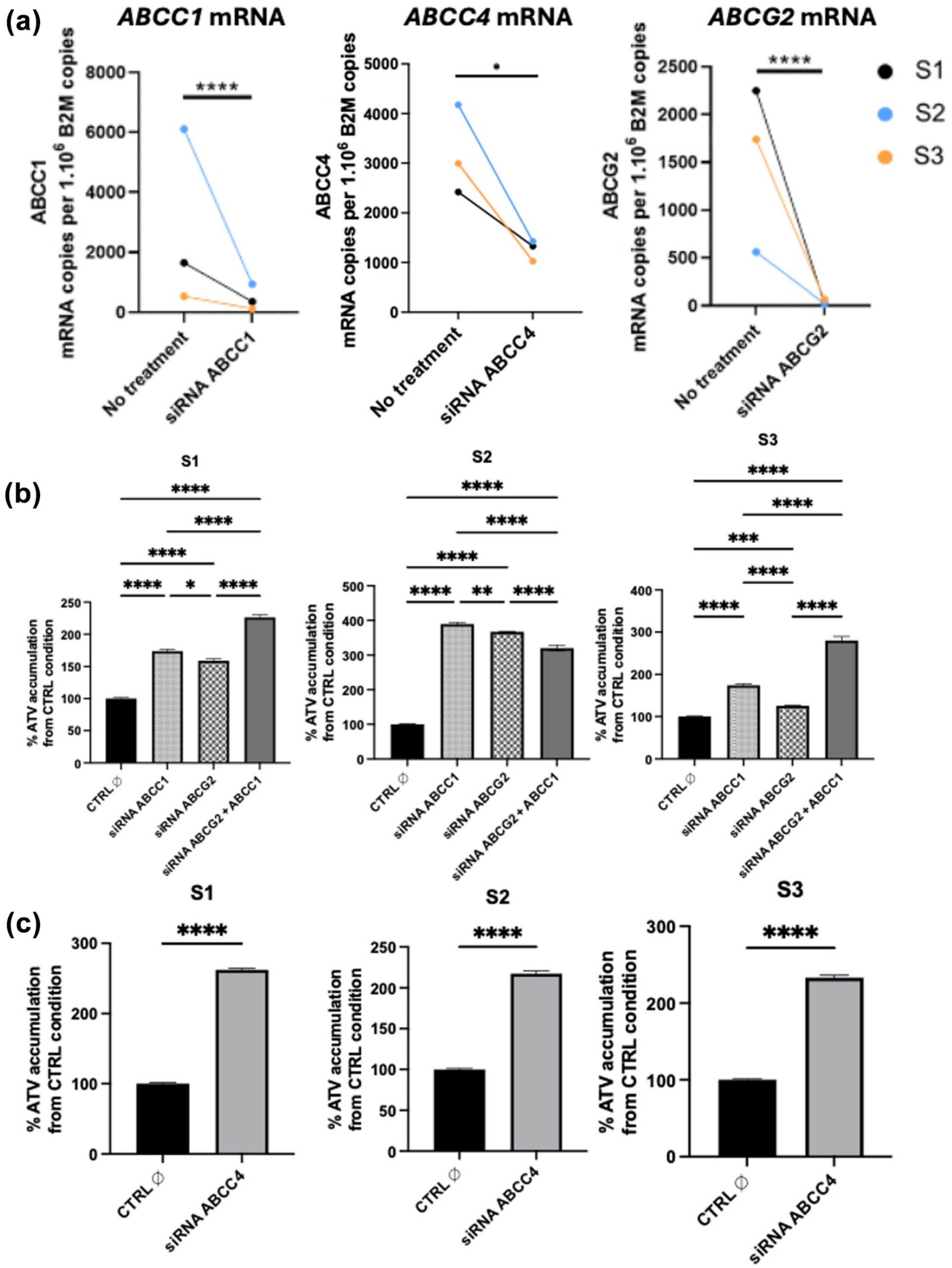


FIGURE 6 Legend on next page.

14765381, 0, Downloaded from https://bpspubs.onlinelibrary.wiley.com/doi/10.1111/bph.17449 by Bibliothecaire En Chef Uni Catholique De Louvain (Ucl), Wiley Online Library on [25/02/2025]. See the Terms and Conditions (https://onlinelibrary.wiley.com/terms-and-conditions) on Wiley Online Library for rules of use; OA articles are governed by the applicable Creative Commons License

ABCG2 WT when compared to HEK293 pCMV controls, whereas the decrease in atorvastatin accumulation observed in HEK293 cells overexpressing the variant (421A) was not significant (Figure 7d). When inhibiting ABCG2 in HEK293 recombinant cell lines with a specific inhibitor (Ko-143 1 μM), we observed that ABCG2 inhibition had no significant impact on intracellular accumulation of atorvastatin in HEK pCMV and ABCG2 variant but increased significantly atorvastatin accumulation in HEK overexpressing the WT protein (Figure 7d).

3.4.2 | Influx transporters

Volunteer selection and modulation of SLCO1B1 *and* SLCO2B1 *expression*

Among influx transporters, *SLCO2B1* was the most expressed at the mRNA level, whereas *SLCO1B1* and *SLCO1B3* were also detected but at low (*SLCO1B1*) and very low (*SLCO1B3*) levels (Figure 2b). To assess their involvement in the intracellular accumulation of atorvastatin, gene silencing experiments with specific siRNA transfections were performed to suppress either *SLCO1B1* or *SLCO2B1* expression in samples from four different volunteers (S4–S7), that is, three per selected gene. Data related to all investigated transporter expression in the four selected volunteers are shown in Figure 8. In the control condition, S5–S7 expressed similar *SLCO1B1* mRNA expression levels. Treatment with *SLCO1B1* siRNA reduced significantly *SLCO1B1* mRNA levels in the volunteers S6 and S7 but not in S5. Considering *SLCO2B1* in the control condition, S4 expressed *SLCO2B1* more importantly than S5 and S6 whose *SLCO2B1* mRNA levels were similar (Figure 9a, Panel A). As expected, *SLCO2B1* siRNA treatment significantly reduced *SLCO2B1* mRNA levels in the samples from all three selected volunteers. The effect at the protein level could not be assessed as no peptide was detected by proteomics, probably due to the low expression and limited sensitivity of our proteomic method.

Effects of SLCO1B1 *and* SLCO2B1 *gene silencing on intracellular accumulation of atorvastatin*

The effects of *SLCO2B1* gene silencing on the intracellular accumulation of atorvastatin was measured in samples from the three volunteers, whereas for *SLCO1B1*, it was analysed only in volunteers whose gene silencing was efficient (i.e., S6 and S7). Treatment with *SLCO1B1* siRNA was associated with a significant decrease in the intracellular concentration of atorvastatin in S7 only (Figure 9a, Panel A). By contrast, counter-intuitively, in S6, treatment with *SLCO1B1* siRNA was associated with a significant increase in the intracellular concentration of atorvastatin. Pooled data from all volunteers are represented in Figure S6c.

After *SLCO2B1* siRNA treatment, the expected reduction of intracellular atorvastatin accumulation was observed in S4, where the expression was the highest in control conditions. Treatment with *SLCO2B1* siRNA in S5 and S6 resulted in a non-significant increase and unchanged atorvastatin intracellular concentrations when compared to the control condition, respectively.

4 | DISCUSSION

The importance of atorvastatin transport into myocytes has been poorly investigated to date. Evidence shows that the dynamics of atorvastatin accumulation in skeletal muscle might play a crucial role in explaining myotoxic events. Very recently, Lauritzen et al. (2023) measured atorvastatin and its metabolites within quadriceps biopsies collected from patients. In this clinical trial, they highlighted an increase in the ATV lactone-to-ATV acid ratio in the skeletal muscle tissue biopsies of the patients experiencing muscle side effects, compared to the ratios in the patients who did not. This observation underscores the significance of atorvastatin transport in explaining muscle toxicities. The lactone form, being highly lipophilic, enters and leaves the cell partly by simple passive diffusion, while the acid form, being less lipophilic, mostly relies on active transporters. This suggests that the transport of atorvastatin acid is relevant to the analysis of the modulation of this ratio. In line with that hypothesis, in their study, Lauritzen et al. demonstrated that correlations between plasma and muscle biopsy concentrations were higher for lactone when compared to acid forms of atorvastatin and its metabolites. However, the published work lacks reliable expression data of transporters within the muscle tissue and the significance of this expression for modulating atorvastatin transport.

In the present study, we found in our screening of the expression of efflux and influx transporters at the mRNA level in the cultured myotubes, a similar trend in the relative transporter expression when compared to open-source databases (GTEx) (Karlsson et al., 2021; The Human Protein Atlas, 2023c). Indeed, our results indicate that *ABCC1* and *SLCO2B1* were the most highly expressed efflux and influx transporters in the cultured differentiated myotubes, respectively. However, the absolute expression levels measured in our study slightly differ from the levels reported in GTEx. For instance, the average *ABCG2* transcript levels were relatively high in our study, that is, only slightly lower than the levels of *ABCC1* mRNA, while in the GTEx depository, *ABCG2* levels were close to zero, demonstrating more important *ABCG2* mRNA levels in the cultured myotubes from our volunteers, compared to open-source databases of 803 biopsy samples. Along the same lines, *SLCO1B1* that was not found to be expressed in skeletal muscle tissues in GTEx, was detected at low expression mRNA levels in the myotubes cultured from all the volunteers assessed here. Different hypotheses could explain those

FIGURE 6 (a) mRNA levels of *ABCC1*, *ABCC4* and *ABCG2* efflux transporters in S1–S3 differentiated myotubes, with or without treatment with siRNAs. (b, c) Intracellular levels of atorvastatin (ATV) in S1–S3 relative to vehicle-treated cells (CTRL) with no treatment (CTRL Ø), treatment with siRNA ABCC1 (siRNA ABCC1), treatment with siRNA ABCG2 (siRNA ABCG2), treatment with siRNA ABCG2 and ABCC1 (siRNA ABCG2 + ABCC1), and treatment with siRNA ABCC4 (siRNA ABCC4). n = 9. **P*<0.05, ***P*<0.01, ****P*<0.001, *****P*<0.0001, significantly different as indicated.

14765381, 0, Downloaded from https://bpspubs.onlinelibrary.wiley.com/doi/10.1111/bph.17449 by Bibliothecaire En Chef Uni Catholique De Louvain (Ucl), Wiley Online Library on [25/02/2025]. See the Terms and Conditions (https://onlinelibrary.wiley.com/terms-and-conditions) on Wiley Online Library for rules of use; OA articles are governed by the applicable Creative Commons License

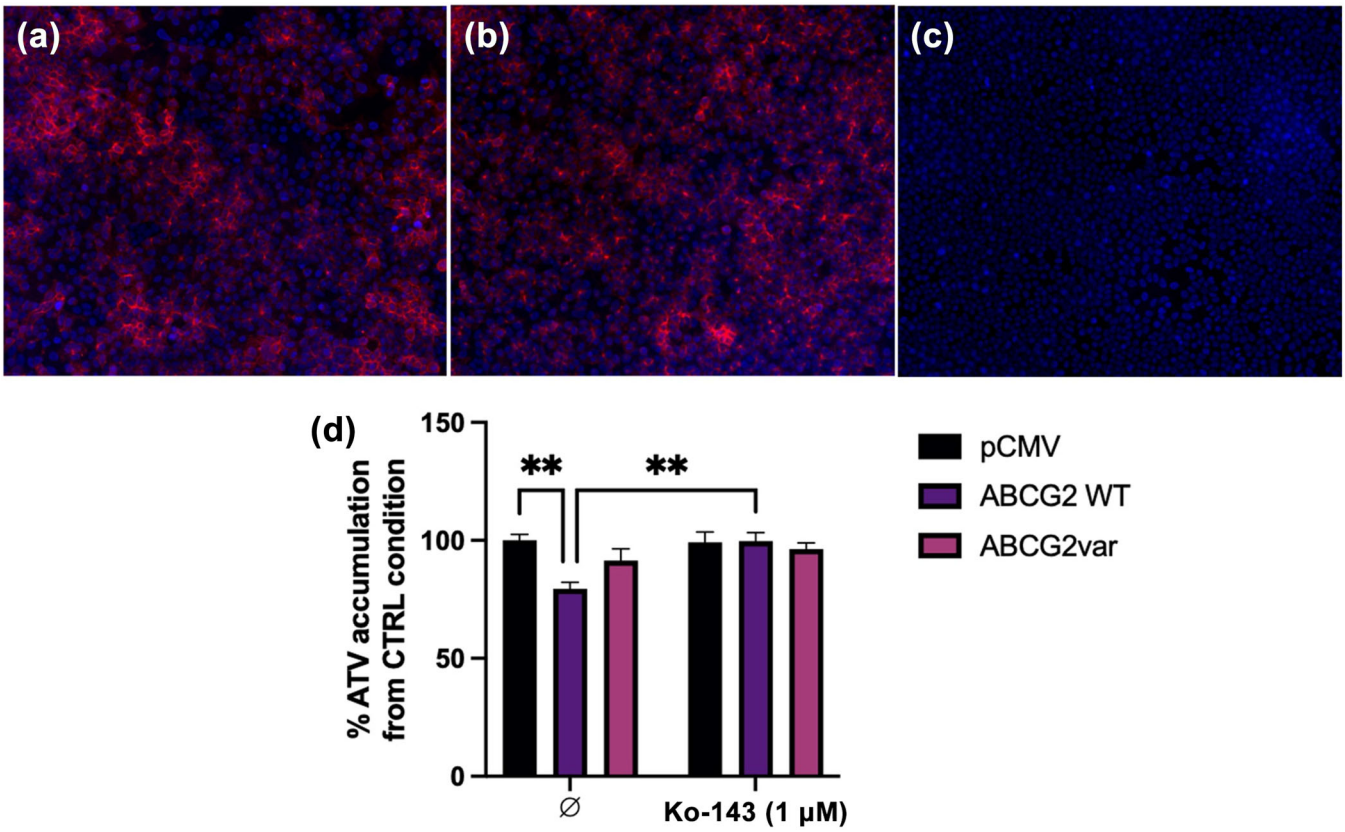


FIGURE 7 (a–c) Overlay of immunofluorescence images (20×) of DAPI nucleus (blue) with PecP ABCG2 (red) of HEK ABCG2 WT (a); HEK ABCG2 variant and HEK pCMV (c) and (d) atorvastatin (ATV) accumulation from CTRL (HEK pCMV) in HEK ABCG2 WT and variant recombinant cell lines with or without Ko-143 inhibition (n = 9). **P<0.01, significantly different as indicated.

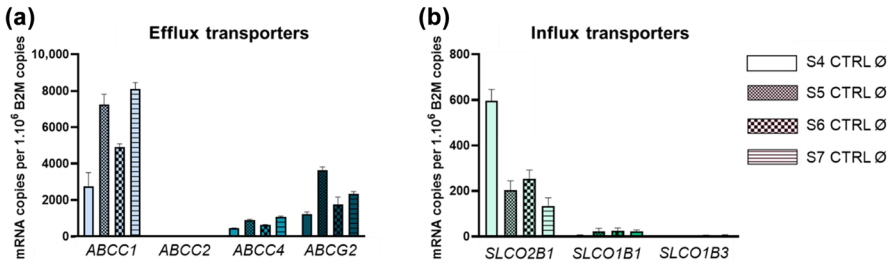


FIGURE 8 Basal mRNA expression of the transporters in control conditions in the volunteers S4–S7 for (a) the efflux transporters and (b) influx transporters.

differences. First, open-source data have been generated directly from muscle biopsies, which comprised various cell types, including muscle fibres but not exclusively. In our study, expression data have been obtained from a primary culture of almost pure differentiated myotubes and might increase the specificity of the measures and the chance to detect a given gene expression. Secondly, in the GTEx project, mRNA quantification was performed by RNA sequencing (RNA-seq), while in our study, we used a targeted RT-qPCR method, generally considered as more specific and sensitive compared to RNA-seq. Therefore, the limit of detection for RT-qPCR is believed to be lower than for RNA-seq, potentially explaining why *SLCO1B1* was not detected in GTEx but was detected in our study. Finally, the environment of cultured myotubes is substantially different from that in vivo. Therefore, expression results in the cultured conditions might not fully be representative of those found in vivo. Overall, our results also indicate a higher level of expression of efflux ABC transporters when compared to influx SLCO carriers, which is in agreement with expression results obtained with biopsies.

Interestingly, not only was *ABCC1* the most expressed transporter gene in differentiated myotubes, but its expression was negatively correlated with intracellular concentrations of atorvastatin. The higher the *ABCC1* mRNA levels, the lower the accumulation of atorvastatin, consistent with an increased efflux of the drug out of the cell when the transporter is more highly expressed. However, this correlation remained no longer statistically significant with ABCC1 protein abundance, even if mRNA levels and protein abundance were correlated.

14765381, 0, Downloaded from https://bpspubs.onlinelibrary.wiley.com/doi/10.1111/bph.17449 by Bibliothecaire En Chef Uni Catholique De Louvain (Ucl), Wiley Online Library on [25/02/2025]. See the Terms and Conditions (https://onlinelibrary.wiley.com/terms-and-conditions) on Wiley Online Library for rules of use; OA articles are governed by the applicable Creative Commons License

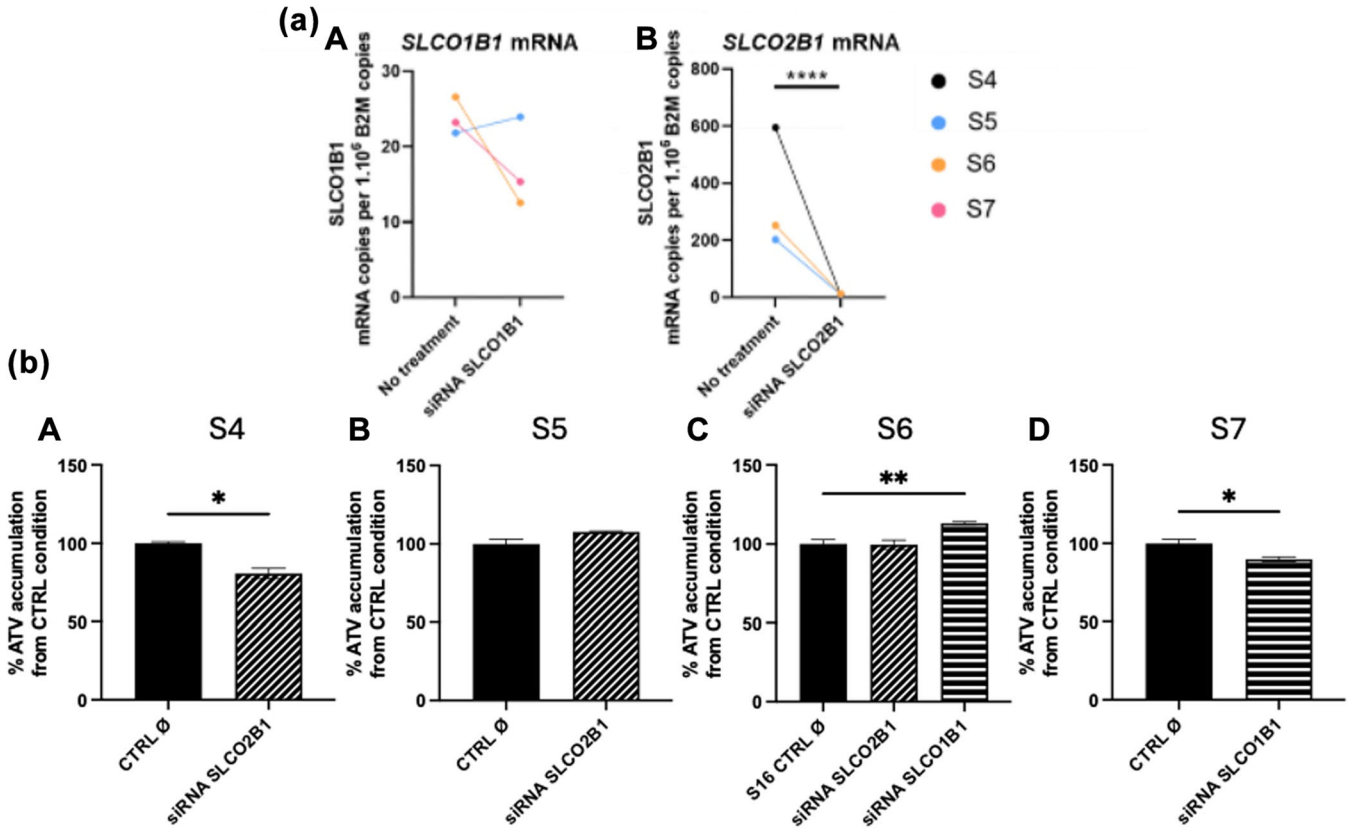


FIGURE 9 (a) Influx transporter mRNA levels (as expressed in mRNA copies per 1.10^6 B2M copies) of (A) *SLCO1B1* and (B) *SLCO2B1* in S4, S5, S6 and/or S7 differentiated myotubes treated or not with siRNA. (b) Intracellular levels of atorvastatin (ATV) relative to vehicle-treated cells (CTRL): (A) S4, (B) S5, (C) S6 and (D) S7. CTRL Ø, no treatment; siRNA SLCO1B1, treatment with siRNA SLCO1B1; siRNA SLCO2B1, treatment with siRNA SLCO2B1. n = 9 for siRNA SLCO2B1 and n = 6 for siRNA SLCO1B1, as data derived from the S5 SLCO1B1 silencing experiment were excluded. **P*<0.05, ***P*<0.01, *****P*<0.0001, significantly different as indicated.

To delve deeper into the causality of the association between transporter expression and modulation of intracellular concentration of atorvastatin, we used molecular (i.e., siRNA) and pharmacological (i.e., transporter inhibitors) approaches. As expected, both the efflux transporter gene silencing and pharmacological inhibition using MK-571 significantly increased intracellular accumulation of atorvastatin, compared to the control condition. Chemical inhibition of OATP1B1/1B3 with CFDA had no significant effect on accumulation of atorvastatin. However, CFDA is also an inhibitor of MRPs, which could have interfered with the influx inhibition effect. Finally, as expected, OATP2B1 inhibition with erlotinib was associated with a decrease in accumulation of atorvastatin, which is consistent with the hypothesis of a diminution of OATP2B1-mediated transport of atorvastatin.

Gene silencing experiments targeting efflux transporters demonstrate that not only ABCC1 but also ABCG2 and ABCC4 can modulate the intracellular transport of atorvastatin under physiological conditions. We also observed that dual *ABCC1–ABCG2* siRNA-induced intracellular accumulation of atorvastatin was higher than the accumulation observed following single siRNA treatment, except in one volunteer who, interestingly, expressed higher *ABCC4* levels and carried the ABCG2 421A variant allele. These observations are consistent with published data, as it has previously been shown that atorvastatin is a substrate for ABCC1, ABCC4 and ABCG2 (Hoste et al., 2023; Knauer et al., 2010). However, those studies assessed atorvastatin in recombinant cellular models where the transporter was overexpressed, compared to the physiological conditions. Here, our results confirm that, at physiological levels of expression, ABC transporter expression has important effects on the cellular transport and accumulation of atorvastatin.

Another potentially interesting observation is that the increase in the intracellular accumulation of atorvastatin with *ABCG2* silencing was relatively low in the myotubes obtained from S3 compared to S1 and S2 volunteers. Based on these data, we genotyped the volunteers and found that this volunteer is a heterozygous carrier of the *ABCG2* variant rs2231142 (c.421C>A, p.Gln141Lys). This suggests that, because ABCG2 activity towards atorvastatin, rather than ABCG2 expression, is already reduced (Cooper-DeHoff et al., 2022; Mirošević Skvrce et al., 2015), silencing the gene expression has only a limited impact on the efflux of intracellular atorvastatin. However, S2 also carries this variant, and the *ABCG2* siRNA-induced increase in the intracellular accumulation of atorvastatin was almost as high as with the *ABCC1* siRNA. To assess the potential effects of *ABCG2* variant rs2231142 (c.421C>A, p.Gln141Lys) on atorvastatin transport, we

14765381, 0, Downloaded from https://bpspubs.onlinelibrary.wiley.com/doi/10.1111/bph.17449 by Bibliothecaire En Chef Uni Catholique De Louvain (Ucl), Wiley Online Library on [25/02/2025]. See the Terms and Conditions (https://onlinelibrary.wiley.com/terms-and-conditions) on Wiley Online Library for rules of use; OA articles are governed by the applicable Creative Commons License

have thus developed a stable recombinant HEK model overexpressing WT or variant *ABCG2* and showed that intracellular accumulation was significantly decreased in HEK293 cells overexpressing ABCG2 WT when compared to HEK293 pCMV controls, whereas the decrease in atorvastatin accumulation observed in HEK293 cells overexpressing the variant (421A) was not significant. This result suggests that the variant affects negatively the protein efflux activity towards atorvastatin, which is in line with the observation that silencing ABCG2 expression in a volunteer 421A-variant carrier had little or no effect on the intracellular accumulation of atorvastatin. In line with this, when inhibiting ABCG2 in HEK293 recombinant cell lines with a specific inhibitor, we observed that ABCG2 inhibition had no significant effect on intracellular accumulation of atorvastatin in pCMV controls and the *ABCG2* 421A variant but significantly increased the accumulation of atorvastatin in HEK cells overexpressing the WT protein. This last observation corroborates our hypothesis that the presence of the *ABCG2* variant affects negatively the efflux activity of the protein, which renders the effects of the ABCG2 inhibition less important in volunteers harbouring this variant. The involvement of the *ABCG2* variant rs2231142 (c.421C>A, p.Gln141Lys) in atorvastatin transport within the muscle tissue has already been suggested in a case–control study where it was associated with 2.9-fold greater odds of developing adverse drug reactions in muscle to atorvastatin (Mirošević Skvrce et al., 2015) without evidence of a clear effect on atorvastatin PK at the systemic level (Birmingham et al., 2015; Keskitalo et al., 2009; Lee et al., 2019; Prado et al., 2018; Tsamandouras et al., 2017). We believe that the higher expression of *ABCG2* in the skeletal muscle, compared with that of *ABCC2* and *SLCO1B1* might explain that, even with no effect on the systemic PK of atorvastatin, the local exposure could influence the drug accumulation and, by extension, the development of muscle side effects. In the hepatocyte, *ABCC2*, which is not expressed in the muscle but is 3.5 times more expressed than *ABCG2* in the liver, might compensate for the reduced *ABCG2* expression/activity (The Human Protein Atlas, 2023a,b) especially because, in the liver, *ABCG2* is about 15 times less expressed than *SLCO1B1* (The Human Protein Atlas, 2023b,d). The reduced hepatic expression of *ABCG2* compared to *SLCO1B1* and *ABCC2* might explain why the effect of the *ABCG2* variant c.421C>A on the systemic PK of atorvastatin is not always detected. Our study shows, in addition, that the modulation of ABCG2 activity/expression might have a different effect when considering the pharmacogenetic background.

Altogether, these results suggest that, in patients, ABCC1, ABCC4 and/or ABCG2 inhibitors might interfere with the local PK of atorvastatin and possibly increase the muscular side effects. While our experimental setting alone cannot fully confirm the link between increased atorvastatin concentrations through cellular transport modulation and clinically relevant toxicity, recent clinical studies and case reports provide compelling evidence supporting this link. Lauritzen et al. found a nearly twofold variation in the ratio of atorvastatin and its metabolites between statin-intolerant and statin-tolerant patients (Lauritzen et al., 2023). Furthermore, cases of severe rhabdomyolysis (Mrotzek et al., 2017) and elevated creatine kinase (Beavers, 2019) have been reported with the concomitant use of atorvastatin and **ticagrelor**, a potent inhibitor of ABCG2. Additionally, in a study conducted in rats, the **probenecid** (ABCC1 inhibitor)-treated group receiving a statin (**rosuvastatin** at a dose of 200 $mg \cdot kg^{-1}$) exhibited up to a 10-fold increase in biological muscle toxicity markers, compared to the groups treated with statin or inhibitor alone (Dorajoo et al., 2008). By extension, it is possible that the concurrent use of ABCC1 inhibitors such as probenecid and **sulfinpyrazone**, ABCG2 inhibitors such as ticagrelor and **elacridar**, HIV protease inhibitors and tyrosine kinase inhibitors or ABCC4 inhibitors such as **celecoxib**, **rofecoxib** and **diclofenac**) with atorvastatin might elevate its intracellular accumulation, potentially heightening the risk of myotoxicities in patients (Liu, 2019) (Table 2). However, further studies with large patient populations are needed to confirm these findings and fully elucidate the link between increased atorvastatin concentration through cellular transport modulation and clinical toxicity.

TABLE 2 Principal inhibitors of investigated ABC transporters adapted from Hasanabady and Kalalinia (2016) and Zhou et al. (2008).

Gene	Protein	Principal inhibitors
ABCC1	MRP1	Probenecid, sulfinpyrazone, **indomethacin**, **verapamil**, **quercetin**, **genistein**, **cyclosporine**, **PAK-104P**, steroid analogues, MK-571, ONO-1078, sulfonylurea, **glibenclamide**
ABCC4	MRP4	MK-571, celecoxib, rofecoxib, diclofenac
ABCG2	BCRP	Ticagrelor, elacridar, HIV protease inhibitors, Ko-143, **fumitremorgin C**, ortataxel, **imatinib**, **nilotinib**, **dasatinib**, **ponatinib**, **lapatinib**, **telatinib**, **sunitinib**, **motesanib**

Results of gene silencing experiments were less marked when considering the influx transporters. Indeed, regarding *SLCO2B1* siRNA treatment, an associated reduction of accumulation was observed in S4 only, whereas little or no effect was observed in S5 and S6, probably because S4 exhibited higher *SLCO2B1* basal expression levels, when compared to others (Figure 6). The anticipated reduction in the intracellular accumulation of atorvastatin with *SLCO1B1* siRNAs was also only observed in one volunteer (S7). Interestingly, S7 exhibited relatively high expression levels of efflux transporters when compared to S6 (Figure 6), where the treatment with *SLCO1B1* siRNA had a counterintuitive effect (i.e., increased accumulation). This observation raises the question of a potential cooperation between influx and efflux transporters in the transport of atorvastatin in the skeletal muscle myotubes. Our hypothesis is that, when the efflux activity is low, simple passive diffusion might be sufficient for the drug to permeate across the cell membrane. Thus, silencing influx transporter expression would have little effect on drug accumulation. By contrast, the role of the influx transporter becomes significant when high efflux activity is present in the cell. In such cases, a slight (10%–20%) decrease in atorvastatin accumulation becomes apparent when the influx transporter expression is suppressed by gene silencing. This hypothesis of the existence of a cooperation between influx and

14765381, 0, Downloaded from https://bpspubs.onlinelibrary.wiley.com/doi/10.1111/bph.17449 by Bibliothecaire En Chef Uni Catholique De Louvain (Ucl), Wiley Online Library on [25/02/2025]. See the Terms and Conditions (https://onlinelibrary.wiley.com/terms-and-conditions) on Wiley Online Library for rules of use; OA articles are governed by the applicable Creative Commons License

efflux transporters is somewhat corroborated by the observation that, in HEK293-transfected (Hoste et al., 2023) and HSMM-transfected (Knauer et al., 2010) cell models, effects of efflux transporters overexpression on the intracellular accumulation of atorvastatin were only observed when the *ABCC1* coding sequence was co-transfected with an influx transporter (SLCO2B1 or rOatp1b2).

Surprisingly, our results demonstrate that silencing the expression of influx transporters had less effect on the cellular levels of atorvastatin than that of efflux transporters. This contrasts with clinical studies evaluating systemic exposure to atorvastatin. Indeed, published reports are unanimous on the importance of OATP1B1 activity for the hepatic excretion of atorvastatin (Niemi, 2007; Ramsey et al., 2023; Stillemans et al., 2022). However, this discrepancy may potentially be explained by the low expression levels of influx transporters in skeletal muscle, compared to those in liver, on the one hand, and compared to the expression of efflux transporters in the muscle, on the other. Secondly, in terms of the systemic excretion, the activity of OATPs in the liver, in cooperation with ABC transporters, generates a vectorial drug transport from the circulating blood into the bile. The situation might thus be viewed differently when considering a 'static' model in which the drug is effluxed to the same environment where the influx is generated.

While the findings gathered with atorvastatin hold significance for other statins, they may not be directly applicable. Other statins, such as **simvastatin** or rosuvastatin, known substrates for some transporters, may exhibit different levels of reliance on these transporters for gaining intracellular access. Furthermore, the lipophilicity, a factor that affects the balance between passive diffusion and transporter-mediated transport, varies among statins. This difference can alter the intracellular accumulation and, as a result, the myotoxic potential (Skottheim et al., 2011).

Our study has, however, some limitations. First, Lipofectamine and the siRNA scramble treatment significantly reduced the expression of the main efflux transporters, compared to the control condition, with no effect on influx transporters (Figures S3 and S4). However, this decrease in efflux transporter expression was less important than the reduction achieved with specific siRNAs and had no significant effect on the intracellular accumulation of atorvastatin (Figure S5). Secondly, even if the proteomic analysis was sensitive enough to quantify ABCC1 and ABCC4 in our samples, no detection was observed for ABCG2, SLCO2B1 and SLCO1B1/1B3. Third, our study may lack statistical power. Theoretically, it is powered enough to detect significant correlations with a rho value greater than |0.6|. Similarly, by using only three to four volunteers for silencing and inhibition experiments, we might miss minor phenotypic consequences, as our design allows for detecting significant differences only for effect sizes (∂) between 0.8 and 1.1. However, due to practical constraints, we were unable to perform functional experiments with multiple conditions in myocytes derived from all 12 biopsies. Instead, we selected volunteers for functional analysis to cover a wide range of expression levels. This selection strategy compensates, at least in part, for the fact that functional analyses were not performed in all volunteers. Finally, we exclusively utilized atorvastatin in its acidic form for our experiments and not its lactone form. Indeed, interconversion between both forms might occur in vivo, and the effects of modulating transporter expression might be different for different ratios of atorvastatin lactone-to- atorvastatin acid.

In conclusion, our study demonstrates that the efflux transporters involved in the cellular transport of atorvastatin are more highly expressed in differentiated myotubes than the influx transporters. By performing in vitro gene silencing in differentiated myotubes and atorvastatin intracellular accumulation experiments in static conditions, we highlight a limited role of influx transporter expression modulation but a major influence of the suppression of efflux ABC transporters on intracellular accumulation of atorvastatin. This second observation could be crucial for explaining drug interactions and statin-related muscle complaints in patients, without an increase in plasma levels. Furthermore, although limited to one observation, our results suggest that pharmacogenetics could confound these results, as c.421C>A *ABCG2* carriers might be less prone to drug–drug interaction involving ABCG2 inhibition.

AUTHOR CONTRIBUTIONS

Emilia Hoste, Vincent Haufroid and Laure Elens designed the research; Louise Deldicque provided and initiated the myotube culture; Emilia Hoste and Nadtha Panin conducted the experiments; Romano Terrasi, Adrien Paquot and Giulio Muccioli performed the HPLC/MS-–MS analysis; Maxime Lingurski and Sébastien Pyr dit Ruys performed the proteomics analysis; Emilia Hoste, Vincent Haufroid, and Laure Elens drafted the manuscript; all authors reviewed and approved the final version of the document.

ACKNOWLEDGEMENTS

The authors thank Dr. Estelle Balan, Dr. Estelle De Groote and Sophie van Doorslaer de Ten Ryen for their help in establishing the protocol in the skeletal muscle cultures. This work was supported by Fonds pour la Formation à la Recherche dans l'Industrie et dans l'Agriculture (FRIA) under Grant FC33437 and by the Bourse du Patrimoine (01150164) to Emilia Hoste and by grants from the Fonds national de la Recherche scientifique (FRS-FNRS) (Grants J018317 and J006920).

CONFLICT OF INTEREST STATEMENT

The authors declare no conflicts of interest.

DATA AVAILABILITY STATEMENT

All datasets used and/or analysed during the current study are available from the corresponding author on reasonable request.

DECLARATION OF TRANSPARENCY AND SCIENTIFIC RIGOUR

This Declaration acknowledges that this paper adheres to the principles for transparent reporting and scientific rigour of preclinical research as stated in the *BJP* guidelines for Design & Analysis and Immunoblotting and Immunochemistry and as recommended by funding agencies, publishers and other organizations engaged with supporting research.

14765381, 0, Downloaded from https://bpspubs.onlinelibrary.wiley.com/doi/10.1111/bph.17449 by Bibliothecaire En Chef Uni Catholique De Louvain (Ucl), Wiley Online Library on [25/02/2025]. See the Terms and Conditions (https://onlinelibrary.wiley.com/terms-and-conditions) on Wiley Online Library for rules of use; OA articles are governed by the applicable Creative Commons License

ORCID

Giulio G. Muccioli https://orcid.org/0000-0002-1600-9259

Laure Elens https://orcid.org/0000-0002-0039-3583

REFERENCES

Adams, S. P., Tsang, M., & Wright, J. M. (2012). Lipid lowering efficacy of atorvastatin. *Cochrane Database of Systematic Reviews*, *12*, Cd008226. https://doi.org/10.1002/14651858.CD008226.pub2

Alexander, S. P., Kelly, E., Mathie, A., Peters, J. A., Veale, E. L., Armstrong, J. F., Faccenda, E., Harding, S. D., Pawson, A. J., Southan, C., Davies, J. A., Amarosi, L., Anderson, C. M. H., Beart, P. M., Broer, S., Dawson, P. A., Hagenbuch, B., Hammond, J. R., Inui, K. I., … Verri, T. (2021). The Concise Guide to PHARMACOLOGY 2021/22: Transporters. *British Journal of Pharmacology*, *178*(Suppl 1), S412–S513. https://doi.org/10.1111/bph.15543

Alexander, S. P. H., Roberts, R. E., Broughton, B. R. S., Sobey, C. G., George, C. H., Stanford, S. C., Cirino, G., Docherty, J. R., Giembycz, M. A., Hoyer, D., Insel, P. A., Izzo, A. A., Ji, Y., MacEwan, D. J., Mangum, J., Wonnacott, S., & Ahluwalia, A. (2018). Goals and practicalities of immunoblotting and immunohistochemistry: A guide for submission to the British Journal of Pharmacology. *British Journal of Pharmacology*, *175*(3), 407–411. https://doi.org/10.1111/bph.14112

Baker, S. K. (2005). Molecular clues into the pathogenesis of statin-mediated muscle toxicity. *Muscle & Nerve*, *31*(5), 572–580. https://doi.org/10.1002/mus.20291

Beavers, J. C. (2019). Elevated creatine kinase due to potential drug interaction with ticagrelor and atorvastatin. *Journal of Pharmacy Practice*, *32*(1), 106–108. https://doi.org/10.1177/0897190017740282

Birmingham, B. K., Bujac, S. R., Elsby, R., Azumaya, C. T., Wei, C., Chen, Y., Mosqueda-Garcia, R., & Ambrose, H. J. (2015). Impact of *ABCG2* and *SLCO1B1* polymorphisms on pharmacokinetics of rosuvastatin, atorvastatin and simvastatin acid in Caucasian and Asian subjects: A class effect? *European Journal of Clinical Pharmacology*, *71*(3), 341–355. https://doi.org/10.1007/s00228-014-1801-z

Cooper-DeHoff, R. M., Niemi, M., Ramsey, L. B., Luzum, J. A., Tarkiainen, E. K., Straka, R. J., Gong, L., Tuteja, S., Wilke, R., Wadelius, M., Larson, E., Roden, D., Klein, T., Yee, S., Krauss, R., Turner, R., Palaniappan, L., Gaedigk, A., Giacomini, K., … Voora, D. (2022). The Clinical Pharmacogenetics Implementation Consortium guideline for *SLCO1B1*, *ABCG2*, and *CYP2C9* genotypes and statin-associated musculoskeletal symptoms. *Clinical Pharmacology and Therapeutics*, *111*(5), 1007–1021. https://doi.org/10.1002/cpt.2557

Curtis, M. J., Alexander, S. P. H., Cirino, G., George, C. H., Kendall, D. A., Insel, P. A., Izzo, A. A., Ji, Y., Panettieri, R. A., Patel, H. H., Sobey, C. G., Stanford, S. C., Stanley, P., Stefanska, B., Stephens, G. J., Teixeira, M. M., Vergnolle, N., & Ahluwalia, A. (2022). Planning experiments: Updated guidance on experimental design and analysis and their reporting III. *British Journal of Pharmacology*, *179*, 3907–3913. https://doi.org/10.1111/bph.15868

De Groote, E., Britto, F. A., Balan, E., Warnier, G., Thissen, J. P., Nielens, H., Sylow, L., & Deldicque, L. (2021). Effect of hypoxic exercise on glucose tolerance in healthy and prediabetic adults. *American Journal of Physiology. Endocrinology and Metabolism*, *320*(1), E43–e54. https://doi.org/10.1152/ajpendo.00263.2020

Demichev, V., Messner, C. B., Vernardis, S. I., Lilley, K. S., & Ralser, M. (2020). DIA-NN: Neural networks and interference correction enable deep proteome coverage in high throughput. *Nature Methods*, *17*(1), 41–44. https://doi.org/10.1038/s41592-019-0638-x

Dorajoo, R., Pereira, B. P., Yu, Z., Gopalakrishnakone, P., Leong, C. C., Wee, A., & Lee, E. (2008). Role of multi-drug resistance-associated protein-1 transporter in statin-induced myopathy. *Life Sciences*, *82*(15–16), 823–830. https://doi.org/10.1016/j.lfs.2008.01.021

European Society of Cardiology. (2022). Cardiovascular realities 2022.

Faul, F., Erdfelder, E., Lang, A. G., & Buchner, A. (2007). G*Power 3: A flexible statistical power analysis program for the social, behavioral, and biomedical sciences. *Behavior Research Methods*, *39*(2), 175–191. https://doi.org/10.3758/bf03193146

Hasanabady, M. H., & Kalalinia, F. (2016). ABCG2 inhibition as a therapeutic approach for overcoming multidrug resistance in cancer. *Journal of Biosciences*, *41*(2), 313–324. https://doi.org/10.1007/s12038-016-9601-5

Hoste, E., Paquot, A., Panin, N., Horion, S., El, H., Muccioli, G. G., Haufroid, V., & Elens, L. (2023). Genetic polymorphisms in *SLCO2B1* and *ABCC1* conjointly modulate atorvastatin intracellular accumulation in HEK293 recombinant cell lines. *Therapeutic Drug Monitoring*, *45*(3), 400–408. https://doi.org/10.1097/FTD.0000000000001043

Karlsson, M., Zhang, C., Méar, L., Zhong, W., Digre, A., Katona, B., Sjöstedt, E., Butler, L., Odeberg, J., Dusart, P., Edfors, F., Oksvold, P., Von, K., Zwahlen, M., Arif, M., Altay, O., Li, X., Ozcan, M., Mardinoglu, A., … Lindskog, C. (2021). A single–cell type transcriptomics map of human tissues. *Science Advances*, *7*(31), eabh2169. https://doi.org/10.1126/sciadv.abh2169

Keskitalo, J. E., Zolk, O., Fromm, M. F., Kurkinen, K. J., Neuvonen, P. J., & Niemi, M. (2009). *ABCG2* polymorphism markedly affects the pharmacokinetics of atorvastatin and rosuvastatin. *Clinical Pharmacology and Therapeutics*, *86*(2), 197–203. https://doi.org/10.1038/clpt.2009.79

Knauer, M. J., Urquhart, B. L., Meyer, H., Schwarz, U. I., Lemke, C. J., Leake, B. F., Kim, R., & Tirona, R. G. (2010). Human skeletal muscle drug transporters determine local exposure and toxicity of statins. *Circulation Research*, *106*(2), 297–306. https://doi.org/10.1161/circresaha.109.203596

Lauritzen, T., Munkhaugen, J., Peersen, K., Kristiansen, O., Sverre, E., Nebauer, S. D., Villseth, M., Andersen, A., Svarstad, A., Jensen, E., Bergan, S., Husebye, E., & Vethe, N. T. (2023). Atorvastatin metabolite pattern in skeletal muscle and blood from patients with coronary heart disease and statin-associated muscle symptoms. *Clinical Pharmacology and Therapeutics*, *113*(4), 887–895. https://doi.org/10.1002/cpt.2844

Lee, N., Maeda, K., Fukizawa, S., Ieiri, I., Tomaru, A., Akao, H., Takeda, K., Iwadare, M., Niwa, O., Masauji, T., Yamane, N., Kajinami, K., Kusuhara, H., & Sugiyama, Y. (2019). Microdosing clinical study to clarify pharmacokinetic and pharmacogenetic characteristics of atorvastatin in Japanese hypercholesterolemic patients. *Drug Metabolism and Pharmacokinetics*, *34*(6), 387–395. https://doi.org/10.1016/j.dmpk.2019.08.004

Liu, X. (2019). ABC family transporters. In X. Liu & G. Pan (Eds.), *Drug transporters in drug disposition, effects and toxicity* (pp. 13–100). Springer Singapore. https://doi.org/10.1007/978-981-13-7647-4_2

Mirošević Skvrce, N., Macolić Šarinić, V., Šimić, I., Ganoci, L., Muačević Katanec, D., & Božina, N. (2015). *ABCG2* gene polymorphisms as risk factors for atorvastatin adverse reactions: A case–control study. *Pharmacogenomics*, *16*(8), 803–815. https://doi.org/10.2217/pgs.15.47

Morikawa, S., Murakami, T., Yamazaki, H., Izumi, A., Saito, Y., Hamakubo, T., & Kodama, T. (2005). Analysis of the global RNA expression profiles of skeletal muscle cells treated with statins. *Journal of Atherosclerosis and Thrombosis*, *12*(3), 121–131. https://doi.org/10.5551/jat.12.121

Mrotzek, S. M., Rassaf, T., & Totzeck, M. (2017). Ticagrelor leads to statin-induced rhabdomyolysis: A case report. *American Journal of Case Reports*, *18*, 1238–1241. https://doi.org/10.12659/ajcr.905974

Niemi, M. (2007). Role of OATP transporters in the disposition of drugs. *Pharmacogenomics*, *8*(7), 787–802. https://doi.org/10.2217/14622416.8.7.787

Norata, G. D., Tibolla, G., & Catapano, A. L. (2014). Statins and skeletal muscles toxicity: From clinical trials to everyday practice. *Pharmacological Research*, *88*, 107–113. https://doi.org/10.1016/j.phrs.2014.04.012

14765381, 0, Downloaded from https://bpspubs.onlinelibrary.wiley.com/doi/10.1111/bph.17449 by Bibliothecaire En Chef Uni Catholique De Louvain (Ucl), Wiley Online Library on [25/02/2025]. See the Terms and Conditions (https://onlinelibrary.wiley.com/terms-and-conditions) on Wiley Online Library for rules of use; OA articles are governed by the applicable Creative Commons License

Ownby, S. E., & Hohl, R. J. (2002). Farnesol and geranylgeraniol: Prevention and reversion of lovastatin-induced effects in NIH3T3 cells. *Lipids*, *37*(2), 185–192. https://doi.org/10.1007/s11745-002-0879-1

Prado, Y., Zambrano, T., & Salazar, L. A. (2018). Transporter genes *ABCG2* rs2231142 and *ABCB1* rs1128503 polymorphisms and atorvastatin response in Chilean subjects. *Journal of Clinical Pharmacy and Therapeutics*, *43*(1), 87–91. https://doi.org/10.1111/jcpt.12607

Preta, G. (2022). Role of lactone and acid forms in the pleiotropic effects of statins. *Pharmaceutics*, *14*(9), 1899. https://doi.org/10.3390/pharmaceutics14091899

Ramsey, L. B., Gong, L., Lee, S. B., Wagner, J. B., Zhou, X., Sangkuhl, K., Adams, S., Straka, R., Empey, P., Boone, E., Klein, T., Niemi, M., & Gaedigk, A. (2023). PharmVar GeneFocus: *SLCO1B1*. *Clinical Pharmacology and Therapeutics*, *113*(4), 782–793. https://doi.org/10.1002/cpt.2705

Sakamoto, K., Honda, T., Yokoya, S., Waguri, S., & Kimura, J. (2007). Rab-small GTPases are involved in fluvastatin and pravastatin-induced vacuolation in rat skeletal myofibers. *The FASEB Journal*, *21*(14), 4087–4094. https://doi.org/10.1096/fj.07-8713com

Skottheim, I. B., Bogsrud, M. P., Hermann, M., Retterstøl, K., & Åsberg, A. (2011). Atorvastatin metabolite measurements as a diagnostic tool for statin-induced myopathy. *Molecular Diagnosis & Therapy*, *15*(4), 221–227. https://doi.org/10.1007/bf03256413

Stillemans, G., Paquot, A., Muccioli, G. G., Hoste, E., Panin, N., Åsberg, A., Balligand, J. L., Haufroid, V., & Elens, L. (2022). Atorvastatin population pharmacokinetics in a real-life setting: Influence of genetic polymorphisms and association with clinical response. *Clinical and Translational Science*, *15*(3), 667–679. https://doi.org/10.1111/cts.13185

Stroes, E. S., Thompson, P. D., Corsini, A., Vladutiu, G. D., Raal, F. J., Ray, K. K., Roden, M., Stein, E., Tokgözoğlu, L., Nordestgaard, B. G., Bruckert, E., De Backer, G., Krauss, R. M., Laufs, U., Santos, R. D., Hegele, R. A., Hovingh, G. K., Leiter, L. A., Mach, F., … European Atherosclerosis Society Consensus Panel. (2015). Statin-associated muscle symptoms: Impact on statin therapy—European Atherosclerosis Society Consensus Panel Statement on Assessment, Aetiology and Management. *European Heart Journal*, *36*(17), 1012–1022. https://doi.org/10.1093/eurheartj/ehv043

The Human Protein Atlas. (2023a). ABCC2. https://www.proteinatlas.org/ENSG00000023839-ABCC2

The Human Protein Atlas. (2023b). ABCG2. https://www.proteinatlas.org/ENSG00000118777-ABCG2

The Human Protein Atlas. (2023c). The Human Protein Atlas. https://www.proteinatlas.org/

The Human Protein Atlas. (2023d). SLCO1B1. https://www.proteinatlas.org/ENSG00000134538-SLCO1B1

Tivnan, A., Zakaria, Z., O'Leary, C., Kögel, D., Pokorny, J. L., Sarkaria, J. N., & Prehn, J. H. M. (2015). Inhibition of multidrug resistance protein 1 (MRP1) improves chemotherapy drug response in primary and recurrent glioblastoma multiforme. *Frontiers in Neuroscience*, *9*, 218. https://doi.org/10.3389/fnins.2015.00218

Tsamandouras, N., Guo, Y., Wendling, T., Hall, S., Galetin, A., & Aarons, L. (2017). Modelling of atorvastatin pharmacokinetics and the identification of the effect of a BCRP polymorphism in the Japanese population. *Pharmacogenetics and Genomics*, *27*(1), 27–38. https://doi.org/10.1097/fpc.0000000000000252

Turner, R. M., Fontana, V., Zhang, J. E., Carr, D., Yin, P., FitzGerald, R., Morris, A., & Pirmohamed, M. (2020). A genome-wide association study of circulating levels of atorvastatin and its major metabolites. *Clinical Pharmacology and Therapeutics*, *108*, 287–297. https://doi.org/10.1002/cpt.1820

Turongkaravee, S., Jittikoon, J., Lukkunaprasit, T., Sangroongruangsri, S., Chaikledkaew, U., & Thakkinstian, A. (2021). A systematic review and meta-analysis of genotype-based and individualized data analysis of *SLCO1B1* gene and statin-induced myopathy. *The Pharmacogenomics Journal*, *21*(3), 296–307. https://doi.org/10.1038/s41397-021-00208-w

UniProt Consortium. (2023). UniProt: The universal protein knowledgebase in 2023. *Nucleic Acids Research*, *51*(D1), D523–d531. https://doi.org/10.1093/nar/gkac1052

Voora, D., Baye, J., McDermaid, A., Narayana, S., Wilke, R. A., Nicole, A., Hajek, C., & Larson, E. A. (2022). *SLCO1B1*5* allele is associated with atorvastatin discontinuation and adverse muscle symptoms in the context of routine care. *Clinical Pharmacology and Therapeutics*, *111*(5), 1075–1083. https://doi.org/10.1002/cpt.2527

Ward, B., Yombi, J. C., Balligand, J. L., Cani, P. D., Collet, J. F., de Greef, J., Dewulf, J., Gatto, L., Haufroid, V., Jodogne, S., Kabamba, B., Pyr, S., Vertommen, D., Elens, L., & Belkhir, L. (2022). HYGIEIA: HYpothesizing the Genesis of Infectious Diseases and Epidemics through an Integrated Systems Biology Approach. *Viruses*, *14*(7), 1373. https://doi.org/10.3390/v14071373

Zhou, S. F., Wang, L. L., Di, Y. M., Xue, C. C., Duan, W., Li, C. G., & Li, Y. (2008). Substrates and inhibitors of human multidrug resistance associated proteins and the implications in drug development. *Current Medicinal Chemistry*, *15*(20), 1981–2039. https://doi.org/10.2174/092986708785132870

SUPPORTING INFORMATION

Additional supporting information can be found online in the Supporting Information section at the end of this article.

How to cite this article: Hoste, E., Deldicque, L., Muccioli, G. G., Panin, N., Terrasi, R., Paquot, A., Lingurski, M., Pyr dit Ruys, S., Haufroid, V., & Elens, L. (2025). Silencing drug transporters in human primary muscle cells modulates atorvastatin pharmacokinetics: A pilot study. *British Journal of Pharmacology*, 1–18. https://doi.org/10.1111/bph.17449

14765381, 0, Downloaded from https://bpspubs.onlinelibrary.wiley.com/doi/10.1111/bph.17449 by Bibliothecaire En Chef Uni Catholique De Louvain (Ucl), Wiley Online Library on [25/02/2025]. See the Terms and Conditions (https://onlinelibrary.wiley.com/terms-and-conditions) on Wiley Online Library for rules of use; OA articles are governed by the applicable Creative Commons License